TABLE 2. Antibodies

Antigen	Dilution	Type of Antibody	Immunized Animal	Company*	Annotation
CK3	×50	Monoclonal	Mouse	PROGEN	Major cytokeratin in corneal epithelium
CK4	×100	Monoclonal	Mouse	Novocastra	Major cytokeratin in non-keratinizing mucosal epithelium
CK12	×100	Polyclonal	Goat	Santa Cruz	Major cytokeratin in corneal epithelium
Muc5AC	×100	Monoclonal	Mouse	Novocastra	Secreted mucin/goblet cell mucin

* PROGEN: Biotechnik GmbH, Heidelberg, Germany; Novocastra: Novocastra Laboratories Ltd., Newcastle, UK; Santa Cruz: Santa Cruz Biotechnology Inc., Santa Cruz, CA.

half of the corneal surface; 3, from one half to three fourths of the corneal surface; 4, more than three fourths of the corneal surface.

Corneal Haze. Grade 0, no haze; 1, trace haze; 2, mild haze easily visible on slit-beam illumination; 3, moderate haze partially obscuring iris details; and 4, marked haze that obscures iris details.

Corneal Neovascularization. Grade 0, no neovascularization and 1, up to 3 clock hours; 2, 3 to 6 clock hours; 3, 6 to 9 clock hours; and 4, >9 clock hours of corneal neovascularization.

Immunostaining and Light-Microscopic Analysis

Two weeks after transplantation, the corneas were excised and further analyzed by histology, immunohistochemistry, and transmission electron microscopy (TEM). Engrafted tissues were removed from the eyes of the 18 rabbits. Normal conjunctival and corneal tissues were also examined for the purpose of comparison. In vivo tissues, cultivated HCjE and HCE cells, and transplanted tissues were divided into two portions, one portion of each of which was embedded in OCT compound (Tissue-Tek; Sakura Fine Technical Co., Ltd.; Tokyo, Japan) and snap frozen with liquid nitrogen for immunostaining analysis. The other portion was processed for TEM.

Immunohistochemistry studies of several tissue-specific cytokeratins in cultivated and transplanted conjunctival and corneal epithelial sheets were performed by previously described methods.[18,20] Tissue sections (8 μm) were placed on silanized slides (Dako Japan, Kyoto, Japan), air dried, and subjected to hematoxylin staining or indirect-immunostaining analysis. The sections were fixed with Zamboni's fixative or acetone (4°C, 5 minutes), incubated for 1 hour in blocking solution (1% BSA in 0.01 M PBS). The sections were incubated at room temperature for 1 hour with primary antibody solutions (Table 2) and normal mouse IgG1, IgG2a, and IgG2b (Dako Japan), and goat IgG (Santa Cruz Biotechnology Inc., Santa Cruz, CA) as negative controls. After they were stained with primary antibodies, the sections were washed with 0.01 M PBS and then treated for 1 hour with the appropriate secondary antibodies: Alexa-488-labeled donkey anti-mouse IgG and Alexa-594-labeled donkey anti-goat IgG (Molecular Probes, Eugene, OR). Subsequently, the sections were washed with 0.01 M PBS and mounted with medium containing an anti-photo-bleaching reagent (3% DABCO; Wako Pure Chemical Industries Ltd., Osaka, Japan). Fluorescent images of the sections were examined by confocal laser microscopy (TCS-SP2; Leica, Tokyo, Japan).

TEM Examination

The specimens were fixed in 2.5% glutaraldehyde in 0.1 M PB, washed three times in PB, and postfixed for 1 hour in 2% aqueous osmium tetroxide. The samples were dehydrated by being passed through a graded ethanol series, transferred to propylene oxide, and embedded in epoxy resin (Epon-812; Shell Chemical, San Francisco, CA). Ultrathin (70 nm) sections were cut and stained with uranyl acetate and counterstained with lead citrate before examination under a TEM (H-7000; Hitachi, Tokyo, Japan).

RESULTS

Histologic Analysis of HCjE and HCE Sheets

Human conjunctival and corneal epithelial cells formed confluent epithelial sheets over the amniotic membranes after 21 days, consisting of five to six layers of well-stratified epithelium, with cuboidal basal cells, and progressive flattening of the cells toward the surface (Fig. 1). TEM examination of the epithelial culture sheet showed that the cells had differentiated into basal columnar cells, suprabasal cuboidal wing cells, and flat squamous superficial cells (Figs. 2A, 2E). Morphologic patterns were similar between cultured conjunctival and corneal epithelia. Numerous microvilli were evident on the surface of the superficial cells (Figs. 2B, 2F), which was almost identical with that found in in vivo corneal epithelium. The basal epithelial cells adhered well to the AM substrate with hemidesmosome attachments (Figs. 2D, 2H), and numerous desmosomal junctions were evident between the epithelial cells in all cell layers (Figs. 2C, 2G).

Transplantation of Cultivated HCjE and Cultivated HCE Sheets

Cultivated HCjE sheets were successfully transplanted onto the corneas of the six rabbits. Complete epithelialization was confirmed by fluorescein staining at the end of surgery. The clinical results of the transplants are summarized in Table 1.

In the group that underwent denuded AM transplantation, four (66.7%) eyes had epithelial defects, and only one (16.7%) eye had a clear cornea. In contrast, four eyes in the HCjE transplantation group had no epithelial defects, and four eyes had clear corneas. These results were comparable to the HCE-transplanted eyes, where similarly, four eyes had no epithelial defects, and five (83.3%) eyes had clear corneas (Fig. 3). For both the HCjE and HCE transplant groups, the epithelial defects were found in eyes in which the contact lens had dislodged or had folded on itself and was abrading the cornea.

Denuded amniotic membrane transplants were associated with significant peripheral corneal neovascularization, with five (83.3%) eyes having grade 4 neovascularization. Cultivated HCjE and HCE transplants were associated with significantly less neovascularization, with only two (33.3%) eyes having grade 2 or 3 neovascularization in each group, and no eyes with grade 4 neovascularization. The majority of corneas that underwent cultivated HCjE transplantation were transparent, smooth, and devoid of epithelial defects 2 weeks after transplantation (66.7%). There were no instances of graft retraction or dislodgement.

Immunohistochemistry

The engrafted HCjE and HCE tissues consisted of five to six layers of stratified epithelial cells, with cuboidal or columnar basal cells and flattened squamous superficial cells. The grafts stained positively for the antihuman nuclei antibody, confirm-

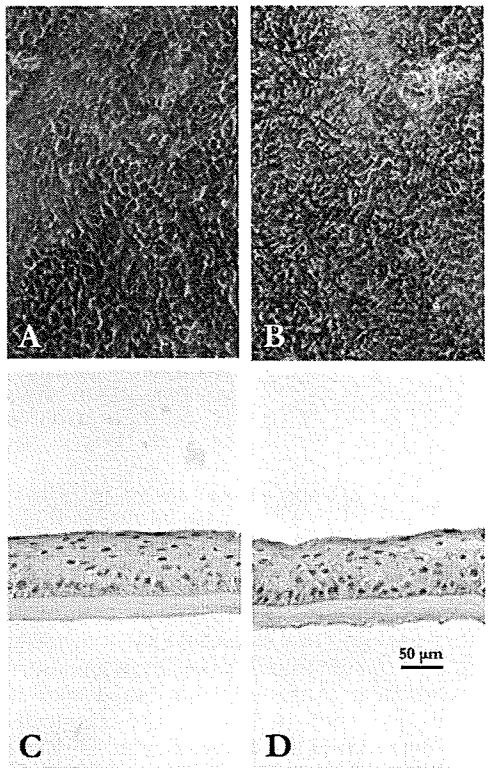

FIGURE 1. Histologic examination: in vitro HCE examined with phase-contrast microscopy (**A**) and light microscopy (**C**) at day 21 of culture. In vitro HCjE examined with phase-contrast microscopy (**B**) and light microscopy (**D**) at day 21 of culture.

ing that the epithelial cells on the rabbit corneas were of human origin. The engrafted cultivated conjunctival epithelium expressed the conjunctiva-specific keratin CK4 which was consistent with engrafted corneal epithelium and also normal in vivo conjunctiva (Figs. 4B, 4E, 4H). Cornea-specific CK12 was seen in both in vivo cornea and engrafted HCE and although it was present only minimally in in vivo conjunctiva, it became more obvious in transplanted conjunctiva. In cultivated (Fig. 4D) and engrafted (Fig. 4G) HCjE, specimens

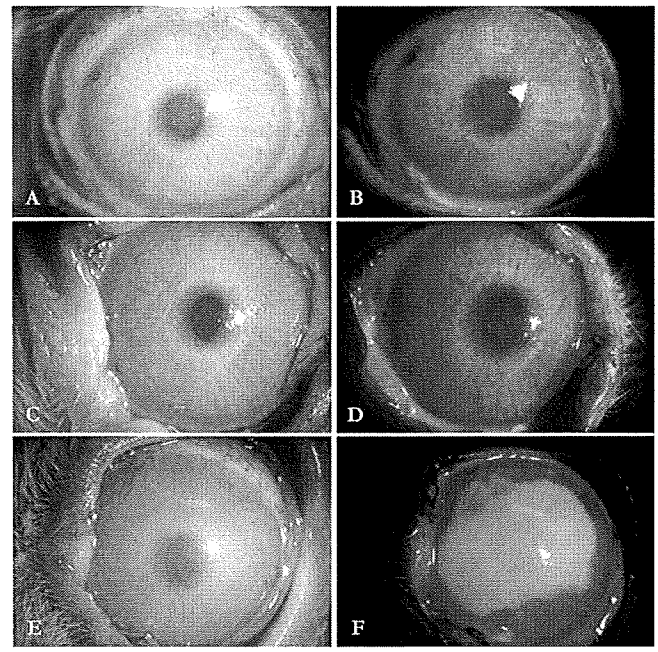

FIGURE 3. Two-week postoperative results: (**A**, **B**) Cultivated conjunctival epithelial transplantation; (**C**, **D**) cultivated corneal epithelial transplantation; and (**E**, **F**) denuded amniotic membrane transplantation.

stained more heavily for cornea-specific keratin 3 than did in vivo conjunctiva (Fig. 4A). This staining pattern was similar to both in vivo and engrafted HCE (Figs. 5A, 5G). Muc5AC staining for goblet cells was absent in both the cultivated HCjE sheet and the engrafted conjunctival epithelium (Figs. 5F, 5I). This result was morphologically similar to that of in vivo corneal epithelium (Fig. 5C).

DISCUSSION

Limbal stem cell transplantation has for the past two decades been the standard treatment for LSCD. However, many patients with severe ocular surface disorders have bilateral disease

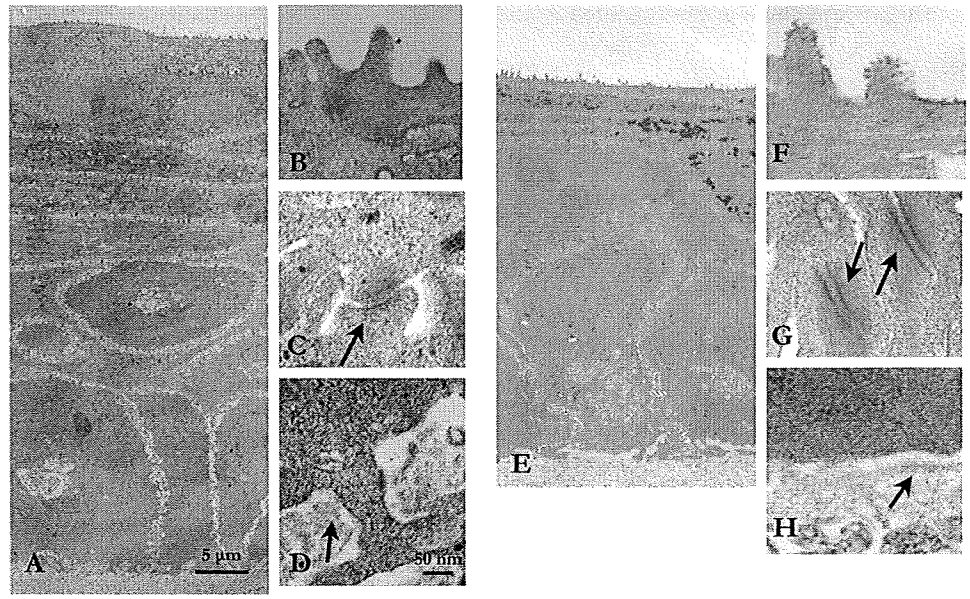

FIGURE 2. TEM of cultured corneal and conjunctival epithelium. Cornea (**A**) and conjunctiva (**E**) at low magnification. Microvilli from HCE (**B**) and HCjE (**F**). Desmosomes (*arrows*) in HCE (**C**) and HCjE (**G**). Hemidesmosome (*arrow*) in HCE (**D**) and (*arrow*) HCjE (**H**).

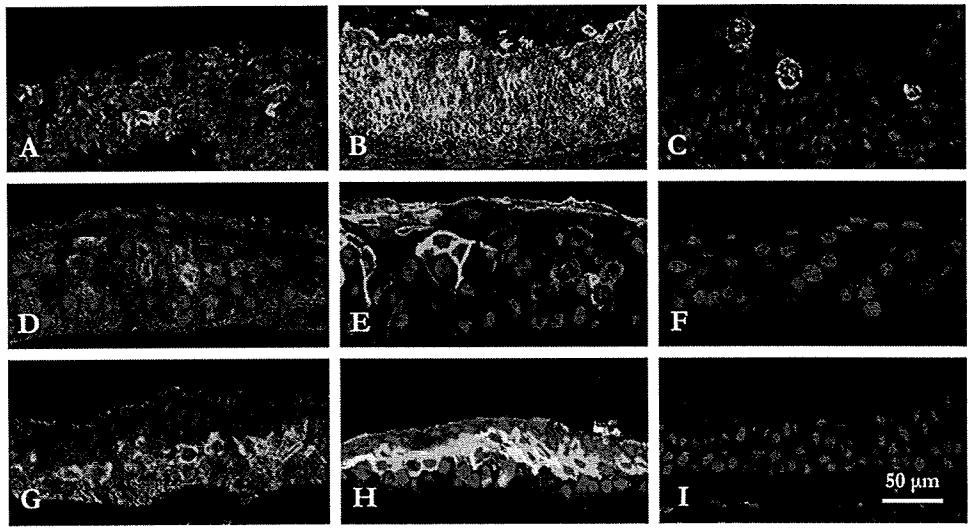

FIGURE 4. Immunohistochemical examination of HCjE. In vivo HCjE (A–C), in vitro HCjE (D–F), and engrafted HCjE (G–I) were immunostained *green* for CK3 (A, D, G), *green* for CK4 and *red* for CK12 (B, E, H), and *green* for Muc5AC (C, F, I).

requiring allogeneic transplantation and long-term immunosuppression, with the attendant systemic risks. In recent years, the use of bioengineered epithelial transplantation has revolutionized the treatment of patients with severe ocular surface disease. The novel use of cultivated autologous conjunctival epithelial transplantation for corneal resurfacing is a promising treatment modality with the advantages that using autologous tissue is safer, has a reduced risk of graft rejection and transmission of infection, and reduces the need for long-term treatment with steroids or immunosuppression. This study demonstrates the effective use of cultivated conjunctival transplantation for corneal epithelial reconstruction and suggests that it may be a viable alternative to cultivated or conventional limbal stem cell transplantation for severe ocular surface disease and severe LSCD.

We recently demonstrated that cultivated conjunctival transplantation may be used for corneal epithelial replacement.[18] The study was focused on morphologic and immunohistochemical characteristics of the cultivated epithelial sheet and showed that cultivated HCjE and the engrafted epithelium manifested five to six layers of stratified squamous epithelium similar in morphology to normal corneal epithelium. The basal cells expressed putative stem cell markers (ABCG2 and P63) and hemidesmosome- and desmosome-component proteins. The cytokeratins CK4, CK13, CK3, and CK12 and the mucin MUC4 were found in the engrafted epithelium.

As an extension of that study, we proceeded to compare the clinical efficacy of cultivated conjunctival transplantation with cultivated corneal and denuded AM transplantation. We showed that transplanted cultivated conjunctiva had clinical results equivalent to that of transplanted cultivated corneal epithelium. The epithelial surface was completely epithelialized, and the corneas remained clear in most of the eyes in both the cultivated conjunctival and cultivated corneal epithelial transplant groups. This result was in contrast to that obtained with denuded amniotic membrane where the majority (66.7%) of eyes had residual epithelial defects with some having large defects and only 16.7% remaining clear. TEM demonstrated the presence of hemidesmosomal attachments of the basal cells and a basal lamina, which are necessary for ensuring graft attachment and integrity after transplantation. The in vitro cultured conjunctival epithelium and engrafted epithelium contained cells that expressed the cornea-specific markers CK3 and CK12. We hypothesize that this was probably derived from clusters of CK3/CK12-positive cells that were present in the in vivo conjunctival tissue. These findings are consistent with our previous report that demonstrated the presence of ectopic clusters of CK3/CK12-positive cells in the conjunctiva.[21]

Our study is the first to compare objectively cultivated human conjunctival transplantation with the current preferred method of cultivated limbal stem cell transplantation. In a

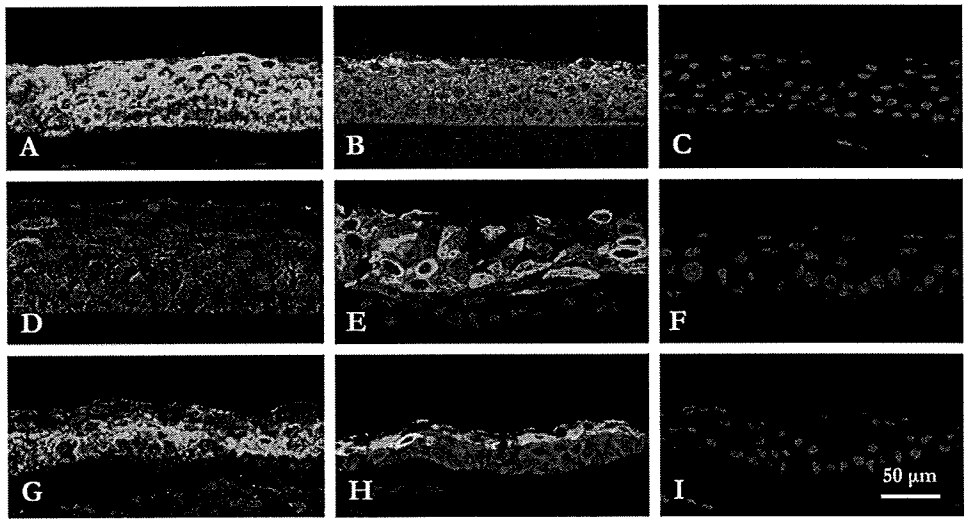

FIGURE 5. Immunohistochemical examination of HCE. In vivo HCE (A–C), in vitro HCE (D–F), and engrafted HCE (G–I) were immunostained *green* for CK3 (A, D, G), *green* for CK4 and *red* for CK12 (B, E, H), and *green* for Muc5AC (C, F, I).

recent study, Ono et al.[22] compared the use of cultivated rabbit conjunctival epithelial transplantation with denuded amniotic membrane transplantation and eyes without any treatment in a limbal-deficiency model. In that study, there was no comparison with cultivated limbal stem cell transplantation, and rabbit tissue was used. As our purpose was to evaluate the clinical feasibility of using cultivated human conjunctival tissue in patients, the use of human tissue would allow us to draw a more direct correlation with the expected clinical results when applied to humans. In addition, using human tissue allowed us to better discriminate between transplanted and migrated host-derived cells, thereby giving us a more objective picture of the true effect of conjunctival transplantation. Our demonstration of the comparable results between cultivated conjunctival and cultivated limbal stem cell transplantation validates the use of conjunctival epithelial transplants as an alternative method of corneal epithelial replacement, while achieving similar good results in terms of ocular surface stability, corneal clarity, and reduction in corneal neovascularization.

In 1989, Kenyon and Tseng[23] described autologous limbal transplantation from the healthy fellow eye as a therapeutic technique for unilateral ocular surface disease. A drawback to this technique was the potential risk of inducing iatrogenic limbal deficiency in the donor eye when too much limbal tissue was removed, as had been previously demonstrated in animal models.[24,25] The potential stem cell depletion in the donor eye secondary to inflammation or subclinical disease has also been reported.[26,27] In cases of bilateral LSCD, treatment with allogeneic limbal epithelium requires the long-term use of steroids and immunosuppression and is associated with systemic complications.[28,29] With the ex vivo expansion technique described herein, only a small amount of autologous conjunctival tissue is required. Even in cases of bilateral involvement, as long as a small amount of healthy conjunctiva was available (1 × 2 mm), we were still able to cultivate an epithelial sheet of sufficient size ex vivo to resurface the corneal defect. With numerous potential sites of harvest,[30–34] there are no significant additional risks should repeat transplantation be required, because of the small amount of tissue needed. In addition, because there is no prior allosensitization, subsequent allografts are not negatively affected (e.g., penetrating keratoplasty).

Eyes with LSCD have persistent epithelial defects and chronic inflammation, and these chronically sick eyes eventually develop conjunctivalization and pannus formation that is usually associated with significant scarring and neovascularization. Denuded amniotic membrane transplantation has also been used for treating these eyes, but as clearly demonstrated in this study, the lack of an intact epithelium results in delayed healing, more inflammation, and more neovascularization compared with an intact epithelium that is simultaneously transplanted. Transplantation of an intact autologous cultured conjunctival epithelium over an amniotic membrane substrate has significant advantages. In contradistinction to the conjunctivalized, vascularized pannus that encroaches on the cornea in LSCD-affected eyes, cultured conjunctival epithelial transplantation involves merely transplanting the conjunctival epithelium without any associated fibrous or vascular tissue. The advantages of having a completely epithelialized surface immediately after transplantation is clearly evident from our study, as it promotes faster recovery, corneal surface stability, and there is less stimulus for conjunctival advancement with accompanying fibrovascular pannus formation. In addition, amniotic membrane transplantation further helps to promote recovery by reducing ocular inflammation, neovascularization, and scarring.

Cultivated oral epithelium has recently been used as an alternative tissue source in the treatment of bilateral severe ocular surface disease. Short- to mid-term results have been encouraging thus far,[9–11] but long-term outcomes are still unknown. Although this method makes use of autologous tissue, oral tissue is of nonocular origin. The use of conjunctiva has several advantages. The cytology and morphology of conjunctival epithelium is more similar to corneal epithelium than that of oral mucosa, thus making it a more favorable tissue source. Significant peripheral neovascularization of oral mucosa–derived grafts has been reported. In certain autoimmune diseases such as ocular cicatricial pemphigoid, oral mucosa theoretically can secrete a common basement membrane target antigen, possibly making it a less desirable tissue source in these groups of patients.[35] Last, the use of endogenous tissue from the eye itself is always preferred over nonocular foreign tissue. In our study, only a minority of eyes that underwent HCjE and HCE transplantation had three or more clock hours of neovascularization. This finding is particularly important in reducing inflammation and scarring, as well as graft rejection or failure in eyes that may subsequently undergo future corneal transplantation. One limitation of our study was the relatively short follow-up duration (14 days) stemming from the use of human grafts in the rabbits, for the reasons we have described. As such, studies with longer observation periods would be necessary, to provide more information on the long-term efficacy of this treatment modality.

In our study, goblet cells were not found in the in vitro and transplanted conjunctival epithelium. The issue of goblet cell differentiation in culture has been a contentious one. Investigators in other studies have demonstrated variable results, with some reports showing the presence[36–38] or absence[39,40] of goblet cells in cultured conjunctival epithelial cells. In many of these studies, rabbit conjunctival epithelium was used. The variability in results may reflect the difference in goblet cell proliferation under various cell culture conditions, such as, if 3T3 cells were in direct contact with cells[36,37] or were in a separate compartment of the culture system,[38–40] if cells were in a submerged condition throughout[36–38] or subjected to air-lifting.[39,40] Goblet cell differentiation is not universal in all studies, and even if present, were usually found to be very scattered and few. In each of these papers, rabbit conjunctival epithelial cells were used. In the present study, we used human conjunctiva, and we exposed cells to air-lifting for 7 days. Under our culture conditions, no distinct Muc5AC-positive cells were present. This variability in results may reflect the relative difficulty in propagating human goblet cells in vitro and may be related to differences in cell culture conditions.

In conclusion, we demonstrated the effective use of cultivated conjunctival transplantation for corneal epithelial replacement in the treatment of total LSCD. This study demonstrated clinically that cultivated conjunctival epithelial transplantation may be a viable alternative to cultivated limbal stem cell transplantation or cultivated oral epithelial transplantation for the treatment of eyes with severe ocular surface disease and limbal deficiency, with the obvious advantages of using an autologous eye tissue source. This finding increases the spectrum of severe ocular surface disorders that can be treated more safely with autologous tissue, as even patients with bilateral disease are likely to have some areas of healthy conjunctival tissue that can be harvested and expanded ex vivo to form a confluent conjunctival sheet. Future studies are needed to assess the long-term efficacy of this procedure.

References

1. Schermer A, Galvin S, Sun TT. Differentiation-related expression of a major 64K corneal keratin in vivo and in culture suggests limbal location of corneal epithelial stem cells. *J Cell Biol.* 1986;103(1):49–62.

2. Cotsarelis G, Cheng SZ, Dong G, Sun TT, Lavker RM. Existence of slow-cycling limbal epithelial basal cells that can be preferentially stimulated to proliferate: implications on epithelial stem cells. *Cell.* 1989;57(2):201-209.
3. Tseng SCG, Chen JJY, Huang AJW, Kruse FE, Maskin SL, Tsai RJF. Classification of conjunctival surgeries for corneal diseases based on stem cell concept. *Ophthalmol Clin North Am.* 1990;3:595-610.
4. Tsubota K, Satake Y, Kaido M, et al. Treatment of severe ocular-surface disorders with corneal epithelial stem-cell transplantation. *N Engl J Med.* 1999;340(22):1697-1703.
5. Solomon A, Ellies P, Anderson DF, et al. Long-term outcome of keratolimbal allograft with or without penetrating keratoplasty for total limbal stem cell deficiency. *Ophthalmology.* 2002;109(6):1159-1166.
6. Samson CM, Nduaguba C, Baltatzis S, Foster CS. Limbal stem cell transplantation in chronic inflammatory eye disease. *Ophthalmology.* 2002;109(5):862-868.
7. Daya SM, Ilari FA. Living related conjunctival limbal allograft for the treatment of stem cell deficiency. *Ophthalmology.* 2001;108(1):126-134.
8. Nakamura T, Endo K, Cooper LJ, et al. The successful culture and autologous transplantation of rabbit oral mucosal epithelial cells on amniotic membrane. *Invest Ophthalmol Vis Sci.* 2003;44(1):106-116.
9. Nishida K, Yamamoto M, Hayashida Y, et al. Corneal reconstruction with tissue-engineered cell sheets composed of autologous oral mucosal epithelium. *N Engl J Med.* 2004;351(12):1187-1196.
10. Nakamura T, Inatomi T, Sotozono C, Amemiya T, Kanamura N, Kinoshita S. Transplantation of cultivated autologous oral mucosal epithelial cells in patients with severe ocular surface disorders. *Br J Ophthalmol.* 2004;88(10):1280-1284.
11. Inatomi T, Nakamura T, Koizumi N, Sotozono C, Yokoi N, Kinoshita S. Midterm results on ocular surface reconstruction using cultivated autologous oral mucosal epithelial transplantation. *Am J Ophthalmol.* 2006;141(2):267-275.
12. Tsai RJ, Li LM, Chen JK. Reconstruction of damaged corneas by transplantation of autologous limbal epithelial cells. *N Engl J Med.* 2000;343(2):86-93.
13. Ang LP, Tan DT, Cajucom-Uy H, Beuerman RW. Autologous cultivated conjunctival transplantation for pterygium surgery. *Am J Ophthalmol.* 2005;139(4):611-619.
14. Ang LP, Tan DT, Beuerman RW, Lavker RM. Development of a conjunctival epithelial equivalent with improved proliferative properties using a multistep serum-free culture system. *Invest Ophthalmol Vis Sci.* 2004;45(6):1789-1795.
15. Ang LP, Tan DT, Phan TT, Beuerman RW, Lavker RM. The in vitro and in vivo proliferative capacity of serum-free cultivated human conjunctival epithelial cells. *Curr Eye Res.* 2004;28(5):307-317.
16. Tan DT, Ang LP, Beuerman RW. Reconstruction of the ocular surface by transplantation of a serum-free derived cultivated conjunctival epithelial equivalent. *Transplantation.* 2004;77(11):1729-1734.
17. Ang LP, Tan DT. Autologous cultivated conjunctival transplantation for recurrent viral papillomata. *Am J Ophthalmol.* 2005;140(1):136-138.
18. Tanioka H, Kawasaki S, Yamasaki K, et al. Establishment of a cultivated human conjunctival epithelium as an alternative tissue source for autologous corneal epithelial transplantation. *Invest Ophthalmol Vis Sci.* 2006;47(9):3820-3827.
19. Koizumi N, Cooper LJ, Fullwood NJ, et al. An evaluation of cultivated corneal limbal epithelial cells using cell suspension culture. *Invest Ophthalmol Vis Sci.* 2002;43(7):2114-2121.
20. Hirai N, Kawasaki S, Tanioka H, et al. Pathological keratinisation in the conjunctival epithelium of Sjögren's syndrome. *Exp Eye Res.* 2006;82(3):371-378.
21. Kawasaki S, Tanioka H, Yamasaki K, Yokoi N, Komuro A, Kinoshita S. Clusters of corneal epithelial cells reside ectopically in human conjunctival epithelium. *Invest Ophthalmol Vis Sci.* 2006;47(4):1359-1367.
22. Ono K, Yokoo S, Mimura T, et al. Autologous transplantation of conjunctival epithelial cells cultured on amniotic membrane in a rabbit model. *Mol Vis.* 2007;13:1138-1143.
23. Kenyon KR, Tseng SC. Limbal autograft transplantation for ocular surface disorders. *Ophthalmology.* 1989;96(5):709-722.
24. Chen JJ, Tseng SC. Corneal epithelial wound healing in partial limbal deficiency. *Invest Ophthalmol Vis Sci.* 1990;31(7):1301-1314.
25. Chen JJ, Tseng SC. Abnormal corneal epithelial wound healing in partial-thickness removal of limbal epithelium. *Invest Ophthalmol Vis Sci.* 1991;32(8):2219-2233.
26. Tan DT, Ficker LA, Buckley RJ. Limbal transplantation. *Ophthalmology.* 1996;103(1):29-36.
27. Basti S, Rao SK. Current status of limbal conjunctival autograft. *Curr Opin Ophthalmology.* 2000;11(4):224-232.
28. Ilari L, Daya SM. Long-term outcomes of keratolimbal allograft for the treatment of severe ocular surface disorders. *Ophthalmology.* 2002;109(7):1278-1284.
29. Solomon A, Ellies P, Anderson DF, et al. Long-term outcome of keratolimbal allograft with or without penetrating keratoplasty for total limbal stem cell deficiency. *Ophthalmology.* 2002;109(6):1156-1166.
30. Pellegrini G, Golisano O, Paterna P, et al. Location and clonal analysis of stem cells and their differentiated progeny in the human ocular surface. *J Cell Biol.* 1999;145(4):769-782.
31. Wei ZG, Wu RL, Lavker RM, Sun TT. In vitro growth and differentiation of rabbit bulbar, fornix, and palpebral conjunctival epithelia. Implications on conjunctival epithelial transdifferentiation and stem cells. *Invest Ophthalmol Vis Sci.* 1993;34(5):1814-1828.
32. Wei ZG, Cotsarelis G, Sun TT, Lavker RM. Label-retaining cells are preferentially located in fornical epithelium: implications on conjunctival epithelial homeostasis. *Invest Ophthalmol Vis Sci.* 1995;36(1):236-246.
33. Nagasaki T, Zhao J. Uniform distribution of epithelial stem cells in the bulbar conjunctiva. *Invest Ophthalmol Vis Sci.* 2005;46(1):126-132.
34. Wirtschafter JD, Ketcham JM, Weinstock RJ, Tabesh T, McLoon LK. Mucocutaneous junction as the major source of replacement palpebral conjunctival epithelial cells. *Invest Ophthalmol Vis Sci.* 1999;40(13):3138-3146.
35. Shortt AJ, Secker GA, Notara MD, et al. Transplantation of ex vivo cultured limbal epithelial cells: a review of techniques and clinical results. *Surv Ophthalmol.* 2007;52(5):483-502.
36. Wei ZG, Sun TT, Lavker RM. Rabbit conjunctival and corneal epithelial cells belong to two separate lineages. *Invest Ophthalmol Vis Sci.* 1996;37(4):523-533.
37. Wei ZG, Lin T, Sun TT, Lavker RM. Clonal analysis of the in vivo differentiation potential of keratinocytes. *Invest Ophthalmol Vis Sci.* 1997;38(3):753-761.
38. Meller D, Dabul V, Tseng SC. Expansion of conjunctival epithelial progenitor cells on amniotic membrane. *Exp Eye Res.* 2002;74(4):537-545.
39. Meller D, Tseng SC. Conjunctival epithelial cell differentiation on amniotic membrane. *Invest Ophthalmol Vis Sci.* 1999;40(5):878-886.
40. Cho BJ, Djalilian AR, Obritsch WF, Matteson DM, Chan CC, Holland EJ. Conjunctival epithelial cells cultured on human amniotic membrane fail to transdifferentiate into corneal epithelial-type cells. *Cornea.* 1999;18(2):216-224.

Investigation of the Corneal Filament in Filamentary Keratitis

Hidetoshi Tanioka, Norihiko Yokoi, Aoi Komuro, Takasumi Shimamoto, Satoshi Kawasaki, Akira Matsuda, and Shigeru Kinoshita

Purpose. To date, no studies have elucidated the composition of the corneal filament in detail. In this study, an immunohistochemical technique was used to clarify the exact composition of the corneal filament in filamentary keratitis. In addition, the mechanisms responsible for filament formation were identified.

Methods. Filaments were obtained from 13 patients with filamentary keratitis with a background of penetrating keratoplasty, aqueous tear deficiency, and severe ocular surface disorders, who were receiving treatment at an outpatient facility. From those tissues, transverse and longitudinal frozen sections were prepared and subjected to an indirect fluorescent immunohistochemical analysis with primary antibodies, including cytokeratins (CK1, -4, -6, -10, -12, and -13), mucins (MUC1, -4, -5AC, and -16), keratinization-related proteins (transglutaminase [TGase]-1 and filaggrin), cell proliferation marker Ki67, and markers of infiltration cells (HLA-DR and neutrophil-elastase). TUNEL staining was used for the detection of apoptosis. Fluorescent images of the sections were inspected with a fluorescence microscope.

Results. The filaments were composed of CK12-positive cells and had a roll-formed central core. They were covered with MUC5AC- and -16-positive mucins including CK4- and -13-positive cells and neutrophil-elastase–positive cells. The filaments also included broken cells and DNA fiber-form postlesional nuclei that were positive for TUNEL staining. However, those areas stained weakly for CK6 and HLA-DR; faintly for CK1, CK10, MUC1, and MUC4; and not at all for Ki67, TGase-1, and filaggrin.

Conclusions. The results of this research have the potential to open new pathways toward understanding the mechanism that generates the filament in filamentary keratitis, as well as new treatments in the future. (*Invest Ophthalmol Vis Sci.* 2009;50:3696–3702) DOI:10.1167/iovs.08-2938

Filamentary keratitis is a chronic disorder of the cornea and, rarely, the conjunctiva, which appears as a variable-length tail extending from the ocular surface epithelium when viewed by slit lamp biomicroscope. The filaments can be stained by rose Bengal, lissamine green, and fluorescein. Patients with filamentary keratitis sometimes experience severe ocular pain. Filamentary keratitis is related to dry eye, especially aqueous-tear–deficient (AQD) dry eye, and it is reportedly associated with various kinds of ocular surface diseases or conditions, such as superior limbic keratoconjunctivitis, acute viral keratoconjunctivitis, postcataract surgery or penetrating keratoplasty (PKP), recurrent erosion, neurotrophic keratopathy, vernal keratoconjunctivitis, prolonged use of an eye patch, ptosis, and large-angle strabismus.[1–6] Filaments are known to be composed of mucin, which is stained by periodic acid-Schiff (PAS) or Alcian blue, and degenerating and regenerating epithelial cells.[7–9] However, only histologic studies by light- or electron microscopy, not by immunohistochemical examination, have been performed on this condition.[7,8,10–12] To date, reported studies regarding filaments are limited to only basic pathologic examination. Therefore, in our present study we used an immunostaining technique to accurately obtain the specific composition of the filaments. In addition, we identified the mechanisms responsible for filament formation.

Methods

Enrollment of Patients

The study involved 13 patients with filamentary keratitis (Table 1) who were receiving treatment for removal of the filaments at an outpatient facility. This research was approved by the Committee for Ethical Issues on Human Research at Kyoto Prefectural University of Medicine and adhered to the tenets of the Declaration of Helsinki.

Sample Collection

Filaments were obtained from 13 patients with filamentary keratitis after the ocular surface of each patient was examined and photographed with a slit lamp biomicroscope (SL-1600; Nidek Co., Ltd., Aichi, Japan). After anesthesia with topical appreciation of 0.4% oxybuprocaine hydrochloride (Benoxil; Santen Pharmaceutical Co., Ltd., Osaka, Japan), the larger firmaments were collected with forceps. The other filaments were then scraped away with a glass stick. Each patient reported that most of the pain had subsided within a few days after removal of the filament. A normal donor cornea, including conjunctiva (keratoconjunctiva), isolated at 5.5 hours postmortem was obtained from SightLife (Seattle, WA). Filaments and keratoconjunctiva were embedded in OCT compound (Tissue-Tek; Sakura Fine Technical Co., Ltd., Tokyo, Japan) and immediately snap frozen with liquid nitrogen for immunostaining.

Immunostaining and Light Microscopic Analysis

Filament and frozen sections of keratoconjunctiva (8 μm) for immunostaining and light microscopic analysis were placed transversely and longitudinally on glass slides and subjected to hematoxylin and eosin (HE) staining or indirect immunostaining analysis. In brief, the sections were fixed with Zamboni's fixative or acetone (4°C, 5 minutes), immersed for 1 hour in blocking solution (1% BSA in 0.01 M PBS), and treated with primary antibody solutions (Table 2) and normal mouse

From the Department of Ophthalmology, Kyoto Prefectural University of Medicine, Kyoto, Japan.

Supported by a Grant-in-Aid for Scientific Research from the Ministry of Education, Science, Culture, and Sports of Japan.

Submitted for publication September 25, 2008; revised February 23, 2009; accepted June 5, 2009.

Disclosure: **H. Tanioka**, None; **N. Yokoi**, None; **A. Komuro**, None **T. Shimamoto**, None; **S. Kawasaki**, None; **A. Matsuda**, None; **S. Kinoshita**, None

The publication costs of this article were defrayed in part by page charge payment. This article must therefore be marked "*advertisement*" in accordance with 18 U.S.C. §1734 solely to indicate this fact.

Corresponding author: Hidetoshi Tanioka, Department of Ophthalmology, Kyoto Prefectural University of Medicine, 465 kajii-cho, hirokoji-agaru, kawaramachi-dori, kamigyo-ku, Kyoto, 602-0841 Japan; htanioka@koto.kpu-m.ac.jp.

Investigative Ophthalmology & Visual Science, August 2009, Vol. 50, No. 8

TABLE 1. Patients and Samples

Patient No.	Filament Location	Number of Filaments Collected	Age	Sex	Underlying Cause of Filament	Current Treatment at Time of Filament Removal	Photos
1	Upper	2	85	F	OCP	AT	Fig. 2
2	Upper	1	50	F	PKP	AT+OFLX+BETA	Figs. 1A, 1B, 3A-C3, 4A-D3, 5A-G1, 6A-C1
3	Upper	2	84	F	OCP	AT+OFLX+FLM+BETA+PSL	Figs. 1C, 1D, 3A-C4, 4A-D4, 5A-G2, 6A-C2
4	Lower	1	60	F	ATD	AT+LVFX+FLM	Figs. 1E, 1F, 3A-C5, 4A-D5
5	Lower	1	54	F	ATD	AT+LVFX+FLM+HYA	Figs. 3D-J, 4E, 4F
6	Lower	2	88	M	ATD	AT+LVFX+FLM	Figs. 5A-G3, 6A-C3
7	Upper	2	77	M	PKP	LVFX+FLM	
8	Upper	1	51	M	VS	LVFX+BETA+OFLXO	
9	Lower	1	78	F	ATD	AT+LVFX+FLM	
10	Lower	1	69	F	ATD	AT+LVFX+FLM	
11	Lower	1	71	F	ATD	AT+LVFX+FLM	
12	Lower	1	58	F	ATD	AT+OFLX+FLM	
13	Lower	1	49	F	ATD	AT+LVFX+FLM	

Upper, behind upper eye lid; Lower, behind lower eye lid; OCP, ocular cicatricial pemphigoid; ATD, aqueous tear deficiency; VS, vitreous surgery; AT, artificial tear; OFLX, 0.3% ofloxacin eye drop; BETA, 0.1% betamethasone sodium phosphate eye drop; FLM, 0.02% fluorometholone eye drop; PSL, prednisolone tablets; LVFX, 0.5% levofloxacin eye drop; HYA, 0.3% sodium hyaluronate eye drop; OFLXO, 0.3% ofloxacin eye ointment.

IgG1, IgG2a, IgG2b (DakoCytomation, Kyoto, Japan), and goat IgG (Santa Cruz Biotechnology Inc., Santa Cruz, CA) as negative controls. After a 1-hour incubation, the sections were washed with 0.01 M PBS and then treated with fluorescent secondary antibody solutions (Alexa-488- or 594-labeled anti-mouse IgG or anti-goat IgG; Invitrogen, Carlsbad, CA). After a 1-hour incubation, the sections were washed with 0.01 M PBS, and the nuclei were stained with propidium iodide or DAPI and mounted with medium containing 3% anti-photo-bleaching reagent (DABCO; Wako Pure Chemical Industries, Ltd., Osaka, Japan). Unless otherwise stated, all incubations were performed at room temperature. Some filaments were embedded in paraffin wax by standard procedures. The paraffin-embedded sections (4 μm) were stained with HE. Fluorescent and HE-stained images of the sections were taken by microscope with a cooled CCD camera (Olympus Corp., Tokyo, Japan). A commercial fluorometric TUNEL system (DeadEnd; Promega, Madison, WI) was used for analysis of apoptosis.

RESULTS

Slit Lamp Examination

Slit lamp examination of the 13 patients with filamentary keratitis revealed filaments of various sizes. Almost all the big filaments found on the patients' corneas were located behind the upper or lower eye lids (Fig. 1E, Table 1). Whole images of these filaments were observable when fingers were used to open patients' lids (Figs. 1A–D, 1F).

TABLE 2. Antibodies

Group	Antigen	Final Concentration μg/mL	Type of Antibody	Immunized Animal	Company	Annotation
Cytokeratins	CK1	0.025	Mo	M	Novocastra	Major cytokeratin in skin epidermis
	CK4	4.5	Mo	M	Novocastra	Major cytokeratin in nonkeratinizing mucosal epithelium
	CK6	1.0	Mo	M	Novocastra	Expressed at wound healing or hyperproliferative situation
	CK10	0.30	Mo	M	Novocastra	Major cytokeratin in skin epidermis
	CK12	2.0	Po	G	Santa Cruz	Major cytokeratin in cornea
	CK13	2.3	Mo	M	Novocastra	Major cytokeratin in nonkeratinizing mucosal epithelium
Mucin	MUC1	3.4	Mo	M	ZYMED	A membrane-bound mucin
	MUC4	1.0	Mo	M	ZYMED	A membrane-bound mucin
	MUC5AC	0.55	Mo	M	Novocastra	Secreted mucin/goblet cell mucin
	MUC16	0.85	Mo	M	Abcam	A membrane-bound mucin
Infiltration cells	HLA-DR	1.7	Mo	M	Dako Cytomation	Marker of macrophage, Langerhans cell
	Neutrophil elastase	0.70	Mo	M	Dako Cytomation	Marker of neutrophil
Proliferation	Ki67	0.93	Mo	M	Dako Cytomation	Cell proliferation marker
Keratinization-related proteins	Transglutaminase-1	5.0	Mo	M	Blogenesis	Enzyme that catalyzes the cross-linking of envelope component proteins
	Filaggrin	0.25	Mo	M	Blogenesis	Serves as matrix for keratin 1/10 aggregation

Mo, monoclonal; Po, polyclonal; M, mouse; G, goat; Novacastra: Novocastra Laboratories, Ltd., Benton Lane, UK; ZYMED: Zymed Laboratories, Inc., South San Francisco, CA; Abcam: Abcam Co. Ltd., Tokyo, Japan; Biogenesis: Biogenesis Ltd., Poole, UK.

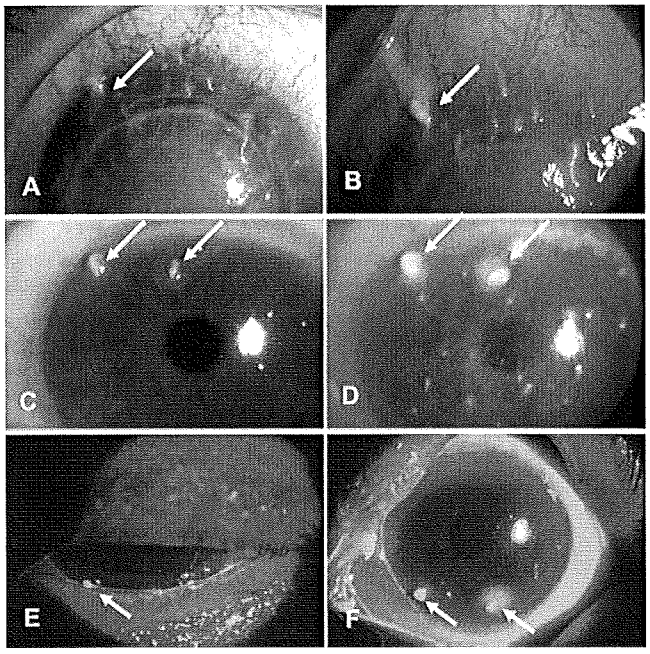

FIGURE 1. Slit lamp examination of filamentary keratitis. The photos are of representative cases of filamentary keratitis. (**A**, **B**) Post-PKP (case 2); (**C**, **D**) ocular cicatricial pemphigoid (case 3) and (**E**, **F**) ATD plus blepharoptosis (case 4). *Arrows*: large filaments.

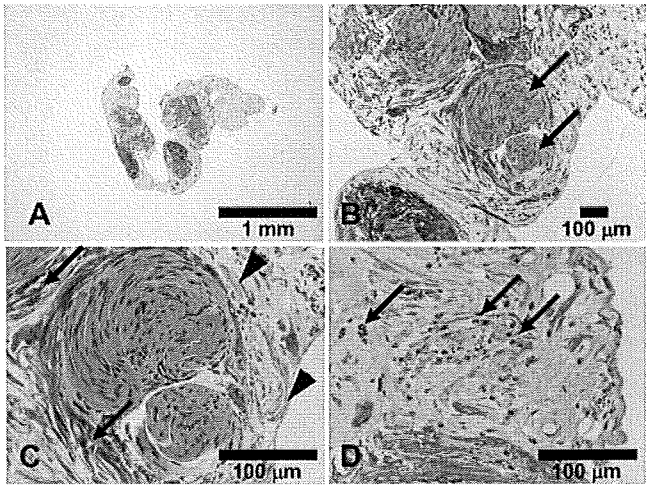

FIGURE 2. Paraffin-embedded HE staining of a filament. A filament taken from the patient with optical cicatricial pemphigoid + blepharoptosis (case 1) was fixed with 10% neutral buffered formalin, embedded in paraffin, sectioned, and stained with HE (hematoxylin eosin) (**A**–**D**). The filament consisted of a core composed of eosinophilic cells that have spindle-shaped cellular cytoplasm and nuclei (*arrows*; **B**). (**C**) The surrounding parts were basophilic fibers (*arrows*) and faint basophilic acellular areas that included basophilic segments (*arrowheads*); (**D**) many cells had polymorphic nuclei (*arrows*).

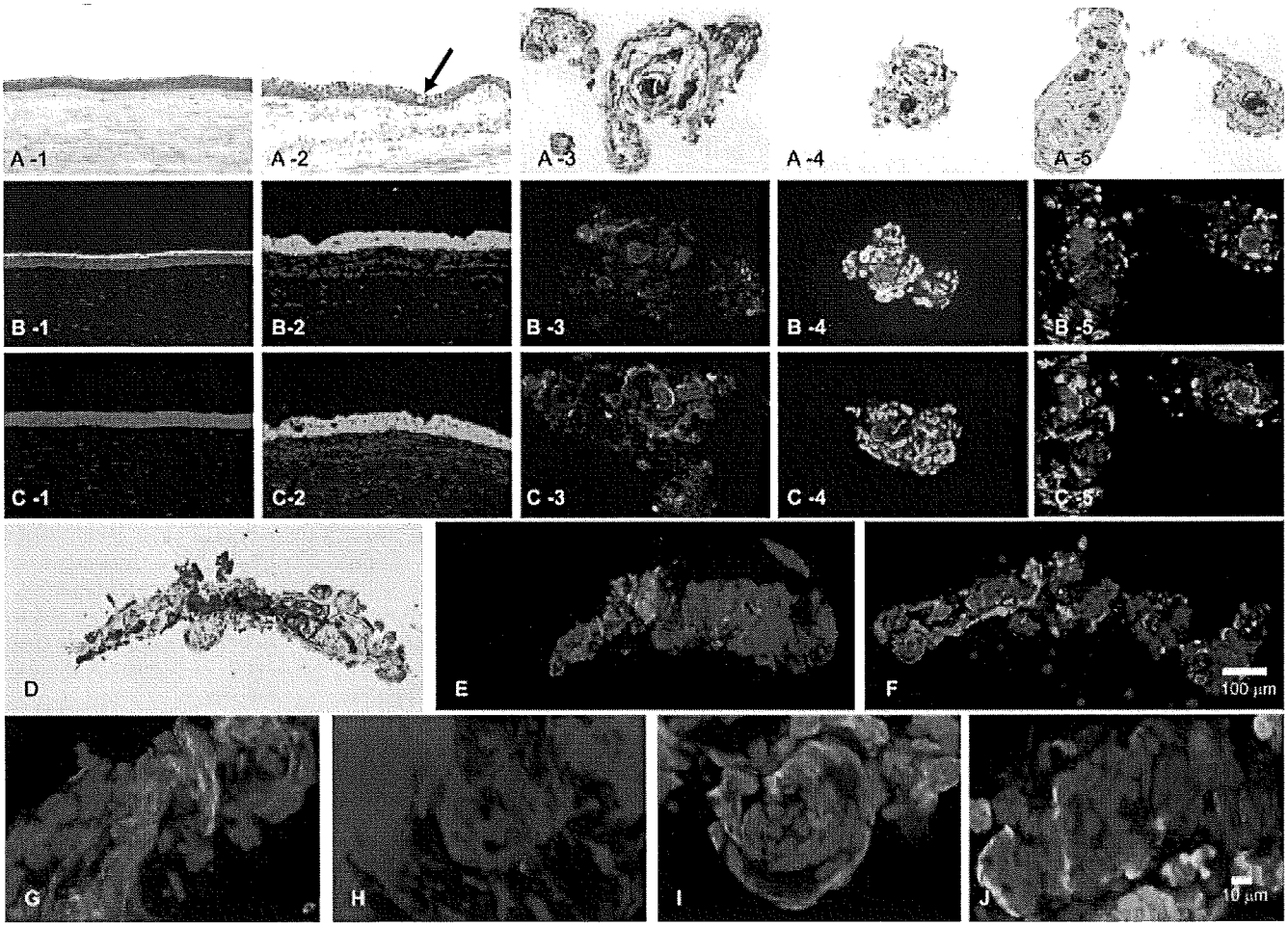

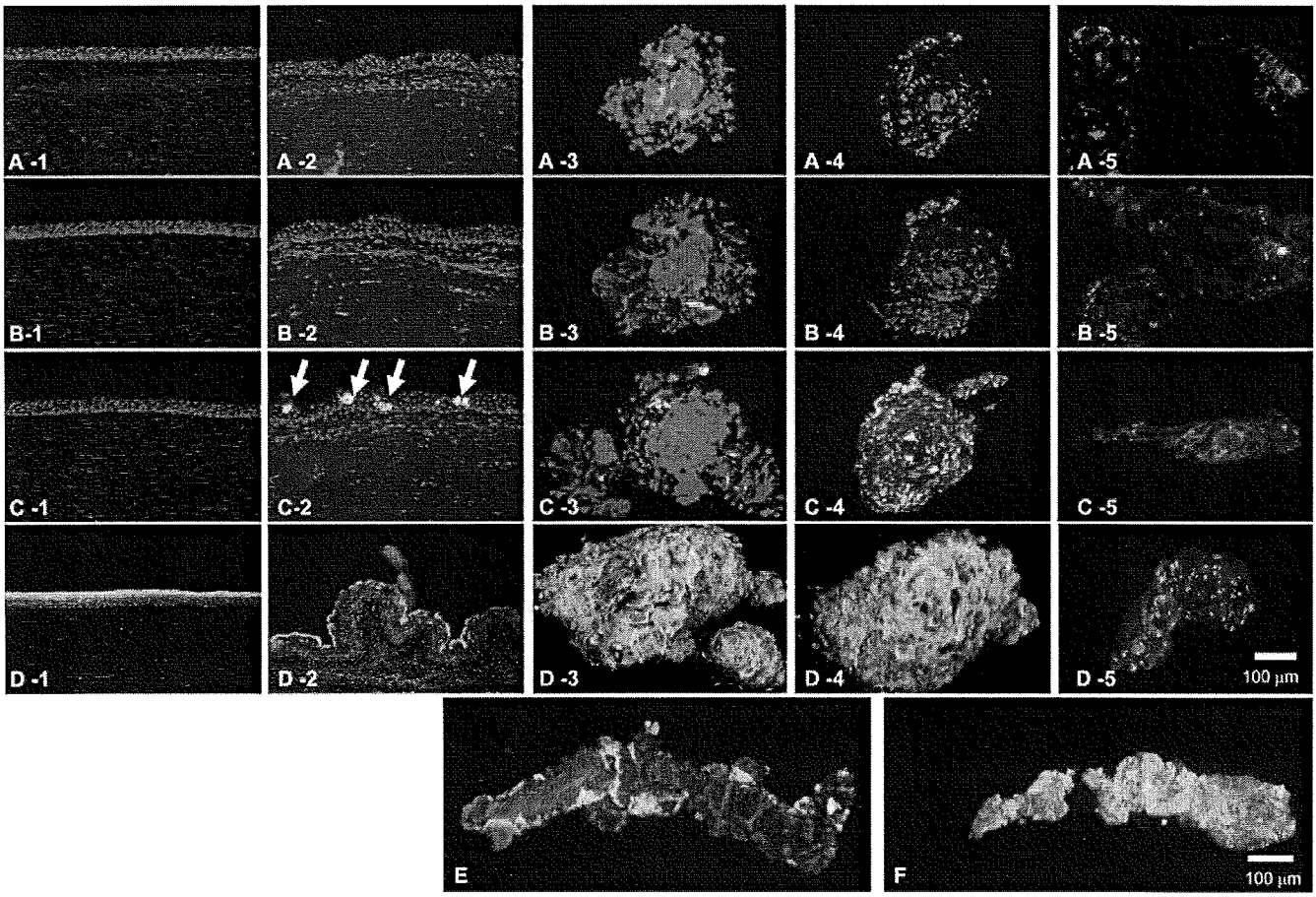

FIGURE 4. The distribution of mucins. (**A**) MUC1/nuclei (*green/red*); (**B**) MUC4/nuclei (*green/red*); (**C, E**) MUC5AC/nuclei (*green/red*); (**D, F**) MUC16/nuclei (*green/red*). (**1**) Corneal epithelium and (**2**) conjunctival epithelium. Filaments in (**3**) a post-PKP eye (case 2), (**4**) an ocular cicatricial pemphigoid eye (case 3), and (**5**) an ATD eye (case 4). Staining for MUC1 and -4 was slightly positive on conjunctival epithelium (**A2, B2**); for MUC5AC was positive on conjunctival epithelium (**C2**) at the goblet cells and the area around the filaments (**C3-5, E**); and for MUC16 was positive on both corneal (**D1**) and conjunctival (**D2**) epithelia and almost all areas of the filaments (**D3-5, F**).

Light Microscopic Analysis

HE staining of paraffin-embedded sections showed that the filament consisted of a core composed of eosinophilic cells that had spindle-shaped cellular cytoplasm and nuclei. The surrounding parts were basophilic fibers and faint basophilic acellular areas that included basophilic segments and polymorphic nucleic cells (Fig. 2). The light microscopic images of HE-stained cryosections of each filament and of normal cornea and conjunctiva showed similar patterns to the patterns shown in the immunostaining images (Figs. 3A1-5). The histologic images of the cryosections were similar to those of the paraffin-embedded sections. The filaments had eosinophilic cores, acellular areas, and basophilic segments. The normal cornea and conjunctiva had eosinophilic epithelium, and a pale goblet cell (Fig. 3A2, arrow) was found in the conjunctival epithelium.

Immunostaining

CK12 was expressed on all layers of normal corneal epithelium. CK4 was expressed on normal conjunctival epithelium and the superficial layer of normal corneal epithelium. Normal conjunctival epithelium was immunostained against CK13 (Fig. 3). In samples that had cores on HE-stained paraffin-embedded and frozen sections (Figs. 2, 3A3-5), the core areas strongly stained red, positive for CK12. In the areas surrounding the filaments, the cellular components strongly stained green, positive for CK4 and -13. A longitudinal section of the filament showed a long core of eosinophilic cells at the center of the filament under HE staining (Fig. 3D). By immunostaining, the red-stained CK12-positive corneal epithelium was found at the center of the filament. These red cores were of an inosculated, ropy, braided shape. The CK4- and -13-positive conjunctival

FIGURE 3. The distribution of the marker of corneal and conjunctival epithelium. (**A, D**) HE staining of the frozen sections (*arrow* indicates a goblet cell); (**B, E, G, H**) CK12/CK4/nuclei (*red/green/blue*); (**C, F, I, J**) CK12/CK13/nuclei (*red/green/blue*); (**A-C**) transverse sections; (**D-J**) longitudinal sections of filament; (**G, H**) magnified view of (**E**); and (**I, H**) magnified view of (**F**). (**1**) Corneal epithelium and (**2**) conjunctival epithelium. Filaments in (**3**) a post-PKP eye (case 2), (**4**) an ocular cicatricial pemphigoid eye (case 3), and (**5**) an ATD eye (case 4). Staining was positive for CK12 on the corneal epithelium (**B1**) and core area of the filaments (**B3-5, C3-5, E, F**); for CK4 on the conjunctival epithelium (**B2**), the superficial epithelium of the cornea (**B1**), and the area around the filaments (**B3-5**); and for CK13 on the conjunctival epithelium (**C2**) and the area around the filaments (**C3-5**). These red cores were of an inosculated, ropy, braided shape (**G, J**). *Blue*: nuclear and DNA fibers.

epithelium, which were stained green, were found in the area around the corneal cells. The side of the attachment site had round or elliptical nuclei stained blue, but the side of the free extremity had a fiber form stained blue by DAPI (Figs. 3D–J). MUC1 and -4 were slightly positive in the conjunctival epithelium, MUC5AC was positive in conjunctival epithelium at the goblet cells, and MUC16 was positive in both the corneal and conjunctival epithelia (Figs. 4A–D1, A–D2). We detected a considerable amount of MUC5AC (goblet-cell–derived, gel-forming mucin) in the acellular area of the filaments, MUC16 (membrane-bound mucin in the corneal and conjunctival epithelium) in almost all areas (Figs. 4C, 4D), but a limited amount of MUC1 and -4 in the filament itself (Figs. 4A, 4B). Moreover, MUC5AC and -16 stained positive in the longitudinal section, and the side of the free extremity had a fiber form that was stained red by PI (Figs. 4E, 4F). Infiltrating cells were positive for neutrophil elastase or HLA-DR. The surrounding areas stained weakly for CK6, which was expressed at wound healing or in a hyperproliferative situation; stained faintly for CK1 and -10, which are major cytokeratins in the epidermis of the skin; and stained not at all for keratinization-related protein (TGase-1 and filaggrin; Fig. 5). The nuclei of the core areas and PI-positive fibrous material around the core were TUNEL positive, but were negative without the rTdT enzyme. These nuclei did not stain for the cell proliferation marker Ki67 (Fig. 6).

Negative control experiments were used for immunostaining under the same conditions used for each antibody, and they showed no positive staining.

A summary of the histological data is shown in Table 3.

Discussion

Wright[8] showed by PAS, Alcian blue, and red oil staining that most of the filaments of filamentary keratitis are composed of mucus with epithelial squamous, lipids, and foreign matter taken up secondarily. Lambert [13,14] reported a theory about the formation of filaments, and that theory has subsequently been included in various textbooks.[2,3] As a normal epithelial surface degenerates due to desiccation, some cells die and fall off, thus leaving a defect. Mucin may adhere to this high-energy pit, and eventually epithelium may grow over the mucin to form a filament. However, Thiel et al.[10] and Zaidman et al.[11] presented another theory pertaining to filamentary keratitis by transmission electron microscopy of a patient with a brain stem disease, which showed that groups of inflammatory cells and fibroblasts were present just below the basal epithelium. It appears that these cells had disrupted the epithelial basement membrane and Bowman's layer. These findings support the theory that filamentary keratitis is associated with the damage of basal epithelial cells, epithelial basement membrane, or both. These findings regarding the components of the filament were derived from classic staining and electron microscopic examination, although they were not enough to completely elucidate the detail and origins of the components. The mechanisms of filament generation that are different from our proposal may be due to these different methods and samples. Therefore, to further elucidate the components of the filament, we examined the filament with an immunostaining technique.

HE staining of the paraffin-embedded sections clearly showed the filament to consist of a core composed of cells that had spindle-shaped, eosinophilic cytoplasm and nuclei. The surrounding parts were basophilic fibers and faint basophilic acellular areas that included basophilic segments and inflammatory cells. Our study revealed that the filament core was composed of corneal epithelium, a finding supported by positive staining for CK12, which is specifically expressed in corneal epithelium. On the other hand, the surrounding portion of the filament was composed mainly of degenerating conjunctival epithelial cells, which had markers typical of conjunctival epithelial cells[15] and did not have markers typical of corneal epithelium. It is also reasonable to speculate that the conjunctival epithelial cells surrounding the filament were mainly derived from the bulbar conjunctival epithelium that is next to the peripheral corneal epithelium and the palpebral

Table 3. Results of Histological Examination

Stain/Antigen	Number	Filament*						
		Core Eosinophilic Spindle-Shaped Cells	Basophilic Fibers	Faint Basophilic Acellular Areas	Basophilic Segment	Polymorphic Nuclei Cells		
HE (Paraffin Section)	1		Basophilic Fibers	Faint Basophilic	Basophilic	Eosinophilic/ Basophilic	Corneal Epithelium	Conjunctival Epithelium
HE (Cryosection)	12	Eosinophilic						
CK12	12	12	–	–	–	–	++	–
CK4	12	–	–	–	12	–	+ (S)	++
CK13	12	–	–	–	12	–	–	++
Muc1	4	–	–	–	4	–	–	+
Muc4	11	–	–	–	11	–	–	+/–
Muc5AC	12	–	–	12	12	–	–	++ (goblet)
Muc16	12	12	–	12	12	–	++ (S)	++ (S)
Neutrophil elastase	11	–	–	–	–	11		
HLA-DR	4	–	–	–	–	4		
CK1	4	4	–	–	–	–		
CK6	4	4	–	–	4	–		
CK10	4	–	–	–	4	–		
Filaggrin	3	–	–	–	–	–		
Transglutaminase-1	3	–	–	–	–	–		
TUNEL	3	3	3	–	3	3		
Ki67	3	–	–	–	–	–		

* Data shown in the Filament are the number that is positive. –, negative; +/–, slightly positive; +, moderately positive; ++, strongly positive; S, superficial.

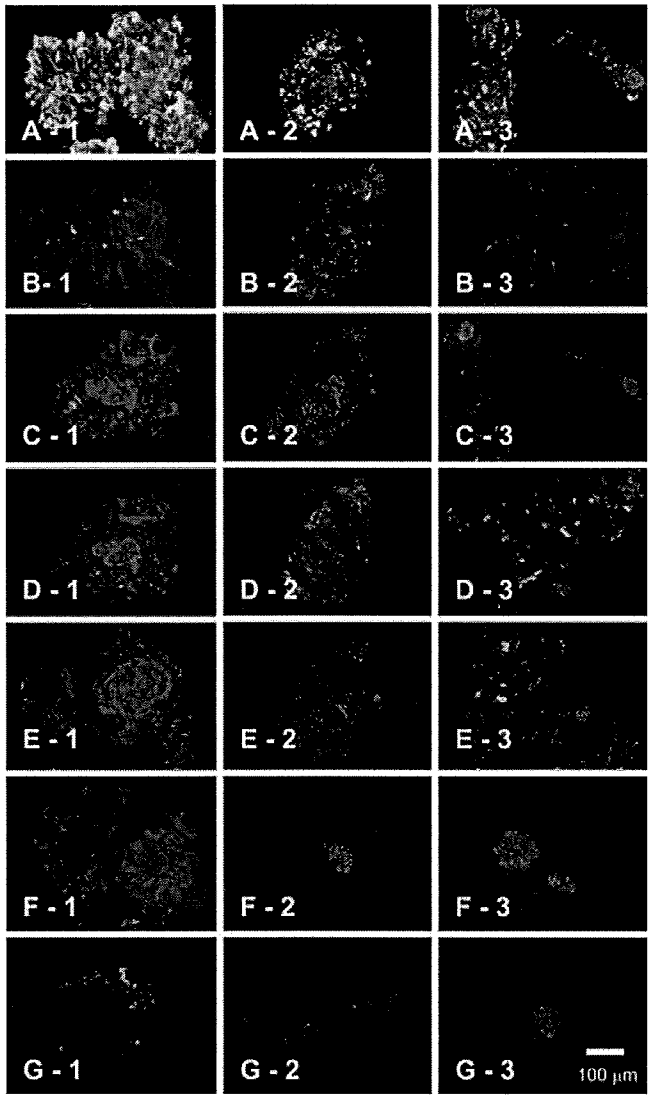

FIGURE 5. Immunostaining of the marker of inflammation cells, keratins, and keratinization-related protein. (**A**) Neutrophil elastase; (**B**) HLA-DR; (**C**) CK1; (**D**) CK6; (**E**) CK10; (**F**) filaggrin; and (**G**) TGase-1. Filaments in (**1**) a post-PKP eye (case 2), (**2**) an optical cicatricial pemphigoid eye (case 3), and (**3**) an ATD eye all stained *green* and the nuclei stained *red* (case 6). The surrounding areas stained for neutrophil-elastase (**A**) and HLA-DR (**B**), stained weakly for CK6 (**D**), stained faintly for CK1 (**C**) and CK10 (**E**), and did not stain at all for keratinization-related protein (**F**, **G**).

conjunctival epithelium that is always in contact with the corneal surface. At the interface between the tear film and ocular surface epithelium, it was demonstrated that membrane-associated mucins, including MUC1, -4, and -16, and a major mucin of the secretory class, the goblet-cell–derived gel-forming MUC5AC, were all present,[16–20] and our study demonstrated that MUC5AC and -16 were the major mucins in the filament. MUC16 is expressed in the superficial corneal epithelium and conjunctival epithelium, and it was found in every part of the filaments in our study. CK1 and -10, although typical of epidermal keratinocytes, have also been described in corneal differentiated cells.[21] Previously, we have shown that the conjunctival epithelium in Sjögren's syndrome expresses the keratinization marker or keratinization-related proteins CK1, CK10, TGase-1, and filaggrin.[22] However, in this study we

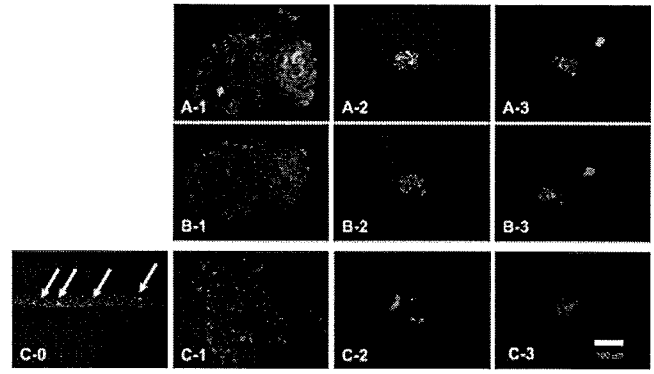

FIGURE 6. TUNEL staining and immunostaining with Ki67. (**A1–3**) TUNEL staining: The nuclei of the core areas and PI-positive fibrous material around the core stained positively for TUNEL, but (**B1–3**) stained negatively without the rTdT enzyme. (**C0**) Some human corneal epithelial cells stained for Ki67 (*arrows*). Filaments of (**C1**) a post-PKP eye (case 2), (**C2**) an optical cicatricial pemphigoid eye (case 3), and (**C3**) an ATD eye (case 6) did not stain clearly for Ki67.

found that those proteins were expressed in the filaments in only a limited amount.

It is also known that filamentary keratitis is often associated with ocular surface inflammation. Our study reaffirmed that association and also demonstrated the existence of neutrophil and HLA-DR-positive cells in the filament. The structural rigidity of the filament, which is assumed to be the result of the twisted form of its core that is additionally supported by the surrounding mucin and the fiber of DNA from postlesional nuclei, is resistant to the condition of repeated friction by the eyelid. Moreover, although it has not been noted in previous reports, the DNA fiber, which exists mainly in the free extremity of the filament and is mixed with mucin, may be essential for the generation of the filament.

Since the large filaments that we were able to collect for this experiment were located behind the upper or lower eye lids, and the core from the corneal epithelium was seen to be of an inosculated, ropy, braided shape, it was thought that the filaments were formed by some mechanical energy. On the ocular surface, we speculate that the mechanical energy was the blinking of the eyelids and/or movement of the eye behind the eyelids.

In summary, although our new theory about the mechanism behind filament generation diverges from that previously reported,[11,13,14] our immunohistologic study of a large number of filament samples obtained from the cornea have led us to the

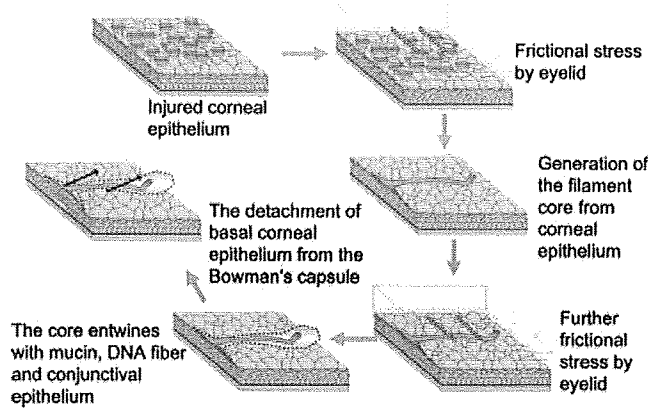

FIGURE 7. Schema for proposed mechanism of filament generation.

following conclusion. We hypothesize that filament generation starts from an injury to the surface epithelium of the cornea due to various disease conditions. Subsequently, friction cause by blinking and/or movement of the eye develops between the palpebral conjunctiva and the injured epithelium and produces the filament core. Further frictional stress is exerted by the eyelid, and the core then entwines with mucin, conjunctival epithelium, fiber of DNA from postlesional nuclei, and inflammatory cells, thus building up the filament. This phenomenon is sometimes associated with inflammation and the detachment of basal cells from the Bowman's layer due to blink- or eye-movement-related mechanical friction (Fig. 7). We believe that the results of this research will open new pathways toward understanding the mechanism that generates the filament in filamentary keratitis, as well as new methods of treatment in the future.

Acknowledgments

The authors thank John Bush for reviewing the article and the Northwest Lion's Eye Bank foundation for helping to obtain fresh human corneal tissues.

References

1. Beetham WP. Filamentary keratitis. *Trans Am Ophthalmol Soc.* 1935;33:413-435.
2. Kinoshita S, Yokoi N. Filamentary keratitis. In: Foster CS, Azar DT, Dohlman CH, eds. *Smolin and Thoft's the Cornea: Scientific Foundations and Clinical Practice*. 4th ed. Philadelphia: Lippincott Williams & Wilkins; 2005.
3. Davidson RS, Mannis MJ. Filamentary keratitis. In: Krachner JH, Mannis MJ, Holland EJ, eds. *Cornea*. 2nd ed. Philadelphia: Elsevier Mosby; 2005.
4. Albietz J, Sanfilippo P, Troutbeck R, Lenton LM. Management of filamentary keratitis associated with aqueous-deficient dry eye. *Optom Vis Sci.* 2003;80:420-430.
5. Diller R, Sant S. A case report and review of filamentary keratitis. *Optometry.* 2005;76:30-36.
6. Kakizaki H, Zako M, Mito H, Iwaki M. Filamentary keratitis improved by blepharoptosis surgery: two cases. *Acta Ophthalmol Scand.* 2003;81:669-671.
7. Maudgal PC, Missotten L, Van Deuren H. Study of filamentary keratitis by replica technique. *Albrecht Von Graefes Arch Klin Exp Ophthalmol.* 1979;211:11-21.
8. Wright P. Filamentary keratitis. *Trans Ophthalmol Soc U K.* 1975; 95:260-266.
9. Tanaka Y, Danjyo S, Hara J, Tanaka R, Minekawa Y. Histological and virological studies of filamentary keratitis following cataract extension [in Japanese]. *Fol Ophthalmol Jpn.* 1983;34:986-990.
10. Thiel HJ, Blumcke S, Kessler WD. Pathogenesis of keratopathia filamentosa (keratitis filiformis): light and electron microscopy study (in German). *Albrecht Von Graefes Arch Klin Exp Ophthalmol.* 1972;184:330-344.
11. Zaidman GW, Geeraets R, Paylor RR, Ferry AP. The histopathology of filamentary keratitis. *Arch Ophthalmol.* 1985;103:1178-1181.
12. Gong H, Hayashida H, Amemiya T. Electron microscopic features of filamentary keratitis [in Japanese]. *Jpn Rev Clin Ophthalmol.* 2000; 94:454-456.
13. Lamberts DW. Dry eye syndromes. In: Foster CS, ed. *Cornea and External Disease*. Chicago: Year Book Medical Publishers; 1985.
14. Lamberts DW. Dry eyes, keratoconjunctivitis sicca. In: Smolin G, Thoft RA, eds. *The Cornea*. 2nd ed. Boston: Little, Brown & Co.; 1987.
15. Wei ZG, Sun TT, Lavker RM. Rabbit conjunctival and corneal epithelial cells belong to two separate lineages. *Invest Ophthalmol Vis Sci.* 1996;37:523-533.
16. Inatomi T, Spurr-Michaud S, Tisdale AS, Gipson IK. Human corneal and conjunctival epithelia express MUC1 mucin. *Invest Ophthalmol Vis Sci.* 1995;36:1818-1827.
17. Inatomi T, Spurr-Michaud S, Tisdale AS, et al. Expression of secretory mucin genes by human conjunctival epithelia. *Invest Ophthalmol Vis Sci.* 1996;37:1684-1692.
18. Inatomi T, Tisdale AS, Zhan Q, Spurr-Michaud S, Gipson IK. Cloning of rat Muc5AC mucin gene: comparison of its structure and tissue distribution to that of human and mouse homologues. *Biochem Biophys Res Commun.* 1997;236:789-797.
19. Gipson IK. Distribution of mucins at the ocular surface. *Exp Eye Res.* 2004;78:379-388.
20. Gipson IK, Inatomi T. Cellular origin of mucins of the ocular surface tear film. *Adv Exp Med Biol.* 1998;438:221-227.
21. Pearton DJ, Ferraris C, Dhouailly D. Transdifferentiation of corneal epithelium: evidence for a linkage between the segregation of epidermal stem cells and the induction of hair follicles during embryogenesis. *Int J Dev Biol.* 2004;48:197-201.
22. Hirai N, Kawasaki S, Tanioka H, et al. Pathological keratinisation in the conjunctival epithelium of Sjögren's syndrome. *Exp Eye Res.* 2006;82:371-378.

Enhancement on Primate Corneal Endothelial Cell Survival In Vitro by a ROCK Inhibitor

Naoki Okumura,[1] *Morio Ueno,*[1,2] *Noriko Koizumi,*[3] *Yuji Sakamoto,*[4] *Kana Hirata,*[3] *Junji Hamuro,*[1] *and Shigeru Kinoshita*[1]

Purpose. The transplantation of cultivated corneal endothelial cells (CECs) has gained attention recently for the treatment of patients with corneal endothelial dysfunction. However, an efficient culturing technique for human (H)CECs has yet to be properly established. The present study was conducted to investigate the applicability of the Rho kinase (ROCK) inhibitor Y-27632 in promoting cultivation of cynomolgus monkey (M)CECs.

Methods. MCECs of cynomolgus monkeys were cultured in a medium containing 10 μM Y-27632. The number of viable cells adherent to culture plates were monitored by a luminescent cell-viability assay and colony growth was detected by toluidine blue staining. Proliferating cells were detected by Ki67 expression using flow cytometry and a BrdU-labeling assay for immunocytochemistry. Annexin V-positive apoptotic cells were analyzed by flow cytometry.

Results. The number of viable cultivated MCECs was enhanced by Y-27632 addition after 24 hours in culture. The colony area of the culture in the presence of Y-27632 was higher than in the absence of Y-27632 on day 10. In Y-27632-treated cultures, the number of Ki67-positive cells was significantly increased at 24 and 48 hours, and the number of proliferating BrdU-positive cells was increased at 48 hours. The number of Annexin V-positive apoptotic cells was decreased at 24 hours.

Conclusions. The inhibition of Rho/ROCK signaling by specific ROCK inhibitor Y-27632 promoted the adhesion of MCECs, inhibited apoptosis, and increased the number of proliferating cells. These results suggest that the ROCK inhibitor may serve as a new tool for cultivating HCECs for transplantation. (*Invest Ophthalmol Vis Sci.* 2009;50:3680-3687) DOI:10.1167/iovs.08-2634

The corneal endothelium is essential for the maintenance of corneal transparency. Since human corneal endothelial cells (HCECs) have poor in vivo proliferative potency, corneal endothelial disorders such as Fuchs' endothelial dystrophy, pseudophakic bullous keratopathy, and trauma lead to a compensatory enlargement of the remaining endothelial cells and irreversible corneal endothelial dysfunction. Penetrating keratoplasty has been widely performed for the improvement of endothelial dysfunction; however, the procedure has several adverse effects such as the potential for irregular astigmatism, suture-induced problems, fragility against trauma, and invasiveness. Alternative methods for replacing the corneal endothelium have been developed, including posterior lamellar keratoplasty, deep lamellar endothelial keratoplasty, and Descemet's-stripping endothelial keratoplasty.[1-3] Although these methods provide considerable benefits clinically, allograft rejection and primary graft failure remain a problem. Moreover, the worldwide shortage of donors is critical. Recently, the transplantation of cultivated CECs has been suggested as an alternative approach to the treatment of corneal endothelial dysfunction. The transplantation of cultured HCECs as a sheet, with[4,5] or without[6] a carrier, and the injection of progenitor cells[7,8] has been explored in animal studies. However, the animal model used in these studies was the rabbit, in which CECs retain high-proliferation ability, and in which residual peripheral CECs proliferate rapidly after injury and regenerate a clear cornea.[9] Aiming to establish a nonhuman primate model with poorly proliferative CECs, we recently reported a cynomolgus monkey model of cultivated CEC sheet transplantation.[10]

However, efficient culture techniques of HCECs need further development before practical application. HCECs are arrested at the G_1-phase of the cell cycle,[11,12] and an age-dependent negative regulation of the cell cycle might causally contribute to the poor proliferative activity in vitro.[13-15] Several studies have reported the successful cultivation of HCECs by use of an animal-derived extracellular matrix (ECM).[16-18]

To establish a clinically applicable efficient way to cultivate HCECs free of animal-origin pathogens, we focused our study on modulating the activity of GTPase Rho, regulating cell-to-substrate and cell-to-cell adhesions.[19-21] Rho and Rho-associated kinases (ROCKs) have a critical function in regulating cell adhesion and cell motility.[22,23] ROCKs are essential in regulating focal adhesions in cultured fibroblasts and epithelial cells.[24] The Rho subfamily contributes to the regulation of many different biological processes through actin-myosin-mediated contractile force generation via the phosphorylation of downstream target proteins.

In terms of other biological effects, Rho GTPases are well known to play a crucial role in cell-cycle progression and in apoptosis. It was initially reported that Rho inactivation blocks G_1-S phase progression and that the microinjection of active RhoA into quiescent cells induces G_1-S phase progression in Swiss 3T3 fibroblasts.[25] Although the underlying mechanism has yet to be thoroughly revealed, ROCK signaling is thought to promote cell-cycle progression in various cell types,[25,26] including CECs.[27] Unlike these reported findings, we have found that inhibition of the ROCK pathway by a selective

From the [1]Department of Ophthalmology, Kyoto Prefectural University of Medicine, Kyoto, Japan; the [2]Department of Ophthalmology, National Center for Geriatrics and Gerontology, Obu, Japan; the [3]Department of Biomedical Engineering Faculty of Life and Medical Sciences, Doshisha University, Kyotanabe, Japan; and the [4]Research Laboratory, Senju Pharmaceutical Co., Ltd., Kobe, Japan.

Supported in part by the Academic Frontier Research Project on the New Frontier of Biomedical Engineering Research and by Grant-in-Aid for Scientific Research 16791076 from the Japanese Ministry of Education, Culture, Sports, Science, and Technology.

Submitted for publication July 29, 2008; revised November 18, 2008, and February 25, 2009; accepted June 22, 2009.

Disclosure: **N. Okumura**, None; **M. Ueno**, None; **N. Koizumi**, None; **Y. Sakamoto**, None; **K. Hirata**, None; **J. Hamuro**, None; **S. Kinoshita**, None

The publication costs of this article were defrayed in part by page charge payment. This article must therefore be marked "*advertisement*" in accordance with 18 U.S.C. §1734 solely to indicate this fact.

Corresponding author: Morio Ueno, Department of Ophthalmology, Kyoto Prefectural University of Medicine, Kyoto 602-0841, Japan; mueno@koto.kpu-m.ac.jp.

Investigative Ophthalmology & Visual Science, August 2009, Vol. 50, No. 8

inhibitor of ROCK, Y-27632, promotes proliferation as well as adhesion of MCECs and inhibits apoptosis.

Materials and Methods

Animal Experiment Approval

In all experiments, animals were housed and treated in accordance with the ARVO Statement for the Use of Animals in Ophthalmic and Vision Research. The experimental procedures were approved by the committee for Animal Research at Kyoto Prefectural University of Medicine.

Primary Cultures

We used eight corneas from four cynomolgus monkeys (3–5 years of age; estimated equivalent human age, 5–20 years) housed at Nissei Bilis Co., Ltd. (Otsu, Japan) and Keari Co., Ltd. (Wakayama, Japan). The corneas were harvested at the time of euthanatization of the monkeys for other research purposes, and the cells were placed in culture within 12 hours. We cultivated MCECs according to a modified protocol of HCEC culture reported previously.[5] Descemet's membrane was stripped of intact MCECs and transferred to 0.6 U/mL of Dispase II (Roche Applied Science, Penzberg, Germany). After a 60-minute incubation at 37°C, the MCECs obtained from individual corneas were resuspended in culture medium and were plated in 1 well of a 12-well plate. All primary cell cultures and serial passages of MCECs were performed in growth medium composed of Dulbecco's modified Eagle's medium (DMEM) supplemented with 10% fetal bovine serum (FBS), 50 U/mL penicillin, 50 μg/mL streptomycin, and 2 ng/mL basic fibroblast growth factor (bFGF; Invitrogen Corp., Carlsbad, CA). MCECs were cultured in a humidified atmosphere at 37°C in 5% CO_2. The culture medium was changed every 2 days. When cells reached confluence in 10 to 14 days, they were rinsed in Ca^{2+} and Mg^{2+}-free Dulbecco's phosphate-buffered saline (PBS), trypsinized with 0.05% trypsin-EDTA (Invitrogen) for 5 minutes at 37°C, and passaged at ratios of 1:2 to 4.

Determination of the Number of Viable Cells

The number of viable cells was determined by a cell-viability assay (CellTiter-Glo Luminescent Cell Viability Assay; Promega Corp., Madison, WI) using the recommended protocol. Viability assays that generate luminescent signals are based on quantification of the ATP levels. MCECs were plated at a density of 2.0×10^3 cells onto 96-well plates. An equal volume of the chemiluminescent reagent was added to 100 μL of medium containing cells for each 96-well plate. Luminescence in each well was measured by a luminometer (Veritas Microplate Luminometer; Turner Biosystems, Sunnyvale, CA) and was standardized to the luminescence of the control. Analyses were performed on the first day of passage and five samples were prepared for each group.

Colony-Forming Efficiency

The clonal growth ability of primary MCECs was determined by the colony-forming efficiency (CFE). Cells were plated at a density of 2.0×10^3 cells/cm^2. Then, the colonies were fixed on day 11 and stained with 0.1% toluidine blue, and the accumulated area was analyzed by Image J software (developed by Wayne Rasband, National Institutes of Health, Bethesda, MD; available at http://rsb.info.nih.gov/ij/index.html). CFEs were expressed as the multiple of change between the control and treated areas. Five samples were prepared for each group.

Immunohistochemistry

Cultured MCECs on chamber slides (Laboratory-Tek; NUNC A/S, Roskilde, Denmark) were fixed in 4% formaldehyde for 10 minutes at room temperature (RT), permeabilized for 5 minutes in PBS containing 0.1% Triton X-100, washed, and incubated for 30 minutes with 1% bovine serum albumin (BSA). For actin studies, the MCECs were incubated at 4°C overnight with a 1:400-dilution rhodamine-conjugated phalloidin molecular probe (Invitrogen) and again washed three times with PBS. For Ki67 and actin double-staining studies, after blocking, the MCECs were incubated at RT with 1:400-dilution rhodamine-conjugated phalloidin (Invitrogen), washed with PBS three times, incubated overnight at 4°C with 1:400-dilution anti-mouse Ki67, and washed again three times. They were then incubated at RT with 1:2000-diluted Alexa Fluor 488-conjugated goat anti-mouse IgG (Invitrogen) and washed three times. During all steps, the endothelial side was face up to avoid damage. After they were washed with PBS in the dark, the specimens were mounted on glass slides with antifade mounting medium containing DAPI (Vector Laboratories, Burlingame, CA), and the slides were inspected with a fluorescence microscope (AX70; Olympus, Tokyo, Japan).

Flow Cytometry Analyses

For Ki67 studies, MCECs prepared as just described were passaged in 1:4 dilutions and cultured for 1 or 2 days. After this, the MCECs were dissociated to single cells by 0.25% trypsin digestion, fixed in 70% (wt/vol) ethanol, washed, and incubated for 20 minutes with 1% BSA. Then, the MCECs were incubated with 1:20-diluted anti-mouse Ki67, washed, and incubated with 1:1000-diluted Alexa Fluor 488-conjugated goat anti-mouse IgG (Invitrogen). For annexin V studies, MCECs were passaged in 1:4 dilutions, and all cells were dissociated to single cells by 0.25% trypsin digestion and recovered, including cells floating in the culture medium, at day 1. They were then subjected to an annexin V assay (Annexin V-FITC Apoptosis Detection Kit Plus; MBL Corp., Nagoya, Japan), according to the manufacturer's instructions. Flow cytometric analyses were then performed (FACSCalibur; BD Biosciences, Franklin Lakes, NJ).

BrdU-Labeling Assay

MCECs prepared as just described were passaged in 1:4 dilutions onto chamber slides (Laboratory-Tek; NUNC A/S), and cultured for 24 hours. They were then incubated for a further 24 hours with 1:1000-diluted 5-BrdU-labeling reagent (Amersham Biosciences, Buckinghamshire, UK). MCEC cultures were next washed in PBS, fixed for 30 minutes in acid-ethanol (90% ethanol; 5% acetic acid; 5% distilled water), washed

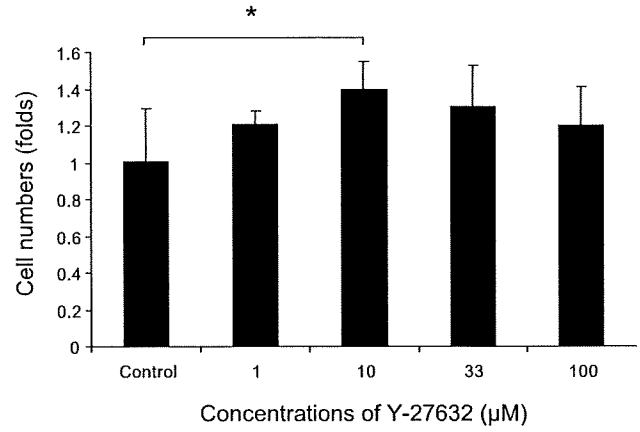

Figure 1. The enhanced survival of primary cultured MCECs by Y-27632. MCECs separated from Descemet's membrane were plated at a density of 2.0×10^3 cells/well in DMEM with 2 ng/mL bFGF. The number of viable MCECs attached to the plate at 24 hours was evaluated by luminescence assay of the ATP levels. Y-27632 at 10 μM resulted in significant cell-survival enhancement (*$P < 0.05$ vs. control). Data are expressed as the ratio to control cells and as the mean ± SE ($n = 5$).

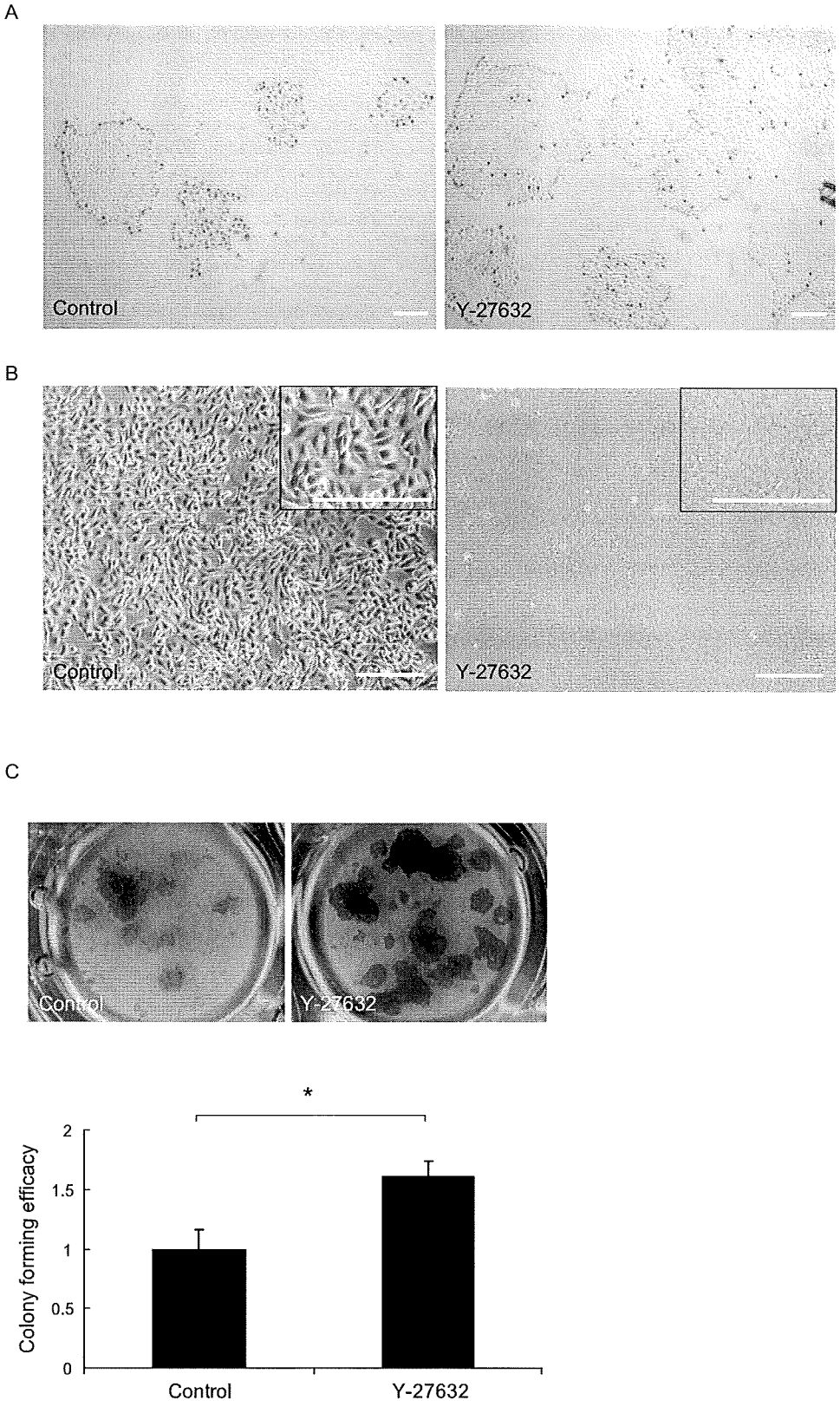

FIGURE 2. The improved culture efficacy of primary MCECs by Y-27632. (**A**, **B**) Primary MCECs from 4-year-old cynomolgus monkeys, prepared as shown in Figure 1, were plated at a density of 2.0×10^4 (**A**) or 2.0×10^5 (**B**) cells/well in the presence or absence of 10 μM Y-27632, and phase-contrast images were analyzed. *Insets*: higher magnification. Scale bar, 250 μm. (**C**) Colony growth of primary cultured MCECs. *Top*: the MCECs, prepared as above, were seeded at a density of 2.0×10^3 cells/cm^2 and stained with 0.1% toluidine blue on day 10. *Bottom*: colony areas of Y-27632-treated cells were elevated compared with those in control cultures (1.6-fold; $^*P < 0.01$). Data are expressed as the mean ± SE ($n = 5$).

with PBS, and incubated with 1% BSA at 37°C for 30 minutes to block nonspecific binding, followed by a 1-hour incubation at RT with mouse anti-BrdU antibody (Amersham Biosciences). After washing, they were then incubated, again at RT, with 1:2000-diluted Alexa Fluor 488–conjugated goat anti-mouse IgG (Invitrogen), washed three times, and mounted on glass slides with antifade mounting medium containing DAPI (Vector Laboratories). The slides were subsequently inspected with a fluorescence microscope.

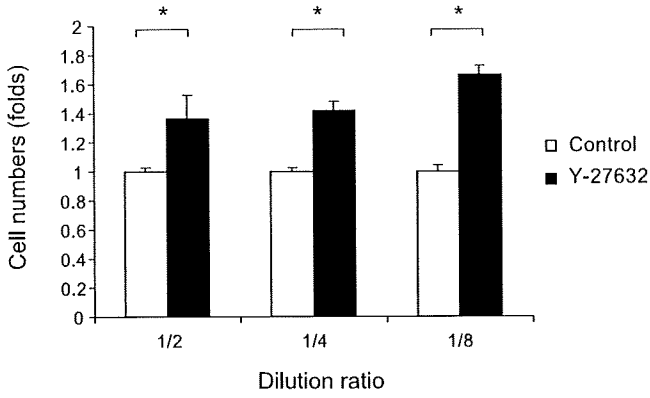

FIGURE 3. Y-27632 augmented the adherence of MCECs during subculture. MCECs, passaged four to six times, were diluted 1:2, 1:4, and 1:8 in the presence of 10 μM Y-27632. Viable cells attached 24 hours after the subculture were determined. The number of viable cells recovered was enhanced significantly in the presence of Y-27632 at all 3 dilutions ($^*P < 0.01$). Data are expressed as the mean ± SE ($n = 5$).

Statistical Analysis

The statistical significance (P) in mean values of the two-sample comparison was determined with Student's t-test. The statistical significance in the comparison of multiple sample sets was analyzed with the Dunnett multiple-comparisons test. Values shown on graphs represent the mean ± SE.

RESULTS

Primary Culture of MCECs

The numbers of viable primary MCECs attached on culture plates 24 hours after the start of the culture were monitored by a luminescent cell-viability assay. The number of viable primary MCECs adherent to the culture plate invariably increased over a wide range of concentrations, from 1 to 100 μM, of Y-27632. A commonly used working concentration of Y-27632,[28] 10 μM, resulted in the highest ($^*P < 0.05$ vs. control) cell-survival enhancement (Fig. 1).

Primary MCECs from 4-year-old cynomolgus monkeys prepared as described earlier were plated at a density of 2.0×10^4 cells/well in a 12-well plate in the presence or absence of 10 μM Y-27632, and phase-contrast images were analyzed. MCECs treated with Y-27632 showed better coverage on day 4 than did the nontreated groups (Fig. 2A). To further confirm the adhesion-improving effect, primary MCECs were seeded at a higher density (2.0×10^5 cells/well) in the presence or absence of 10 μM Y-27632. On day 3, untreated MCECs were proliferating and were enlarged, but were not confluent or homogeneously hexagonal. In contrast, Y-27632-treated MCECs exhibited a confluent monolayer of homogeneously hexagonal cells with smaller sizes (Fig. 2B). For an examination of the distinction of colony growth of primary MCECs between two culture groups with or without Y27632, MCECs were plated at a lower density of 2.0×10^3 cells/well in a 96-well microplate. On day 10, MCECs treated with Y-27632 demonstrated a markedly enhanced increase in colony growth, detected by toluidine blue staining (Fig. 2C). The colony area of Y-27632-treated cells was significantly higher than the control (1.6-fold, $^*P < 0.01$).

Subculture of MCECs

The number of viable primary MCECs adherent to the culture plate was invariably increased in the presence of Y-27632, indicating that there is a possibility that the application of Y-27632 may also improve the CFE of HCECs. To confirm the effect of Y-27632 during the culture passage, we next investigated the effect of Y-27632 on subcultured MCECs. Cultivated cells passaged 4 to 6 times in the presence of Y-27632 were diluted at three dilutions (1:2, 1:4, and 1:8), and the number of viable cells attached on the noncoated culture plate at 24 hours of subculture was then determined. It was found that the number of viable cells recovered was enhanced in the presence of Y-27632 at all three dilutions ($P < 0.01$; Fig. 3). It is of note that the enhancement ratio of adhesion to the plate tends to be higher at higher dilutions during passage. MCECs treated with Y-27632 during subculture showed enhanced cell adhesion both in phase-contrast images and in images of actin fibers immunostained with phalloidin antibody (Fig. 4).

The Effect of Y-27632 on Cell-Cycle Progression

Studies were conducted to determine whether Y-27632 might play a role in cell-cycle progression in MCECs. To answer this question, we first used immunostaining with the cell-cycle population marker Ki67. MCECs at confluence were passaged in 1:4 dilutions and subcultured for 1 or 2 days and were dissociated to single cells by trypsin digestion. MCECs subcultured in the culture medium with Y-27632 showed the presence of a larger number of Ki67-positive cells than was present in the controls (Fig. 5A). Actin immunostaining was also performed to determine whether there is a relationship between Ki67-positive cells and enhanced actin-fiber progression. It turned out that Ki67 expression had no direct relation to actin fibers. Further quantitative flow cytometric analysis revealed the increased presence of Ki67-positive cells in MCECs cultured with Y-27632, 2 days after subculture (Fig. 5B). A BrdU-labeling assay of 48-hour subcultures is shown in Figure 5C, and it shows a larger number of BrdU-positive MCECs among cell populations cultured with Y-27632 compared with control cells. Thus, it was demonstrated that Y-27632 plays a relevant role in the cell-cycle progression of MCECs.

The Effect of Y-27632 on Apoptosis

We next studied the involvement of Y-27632 in apoptosis. MCECs were passaged in 1:4 dilutions at the time of culture

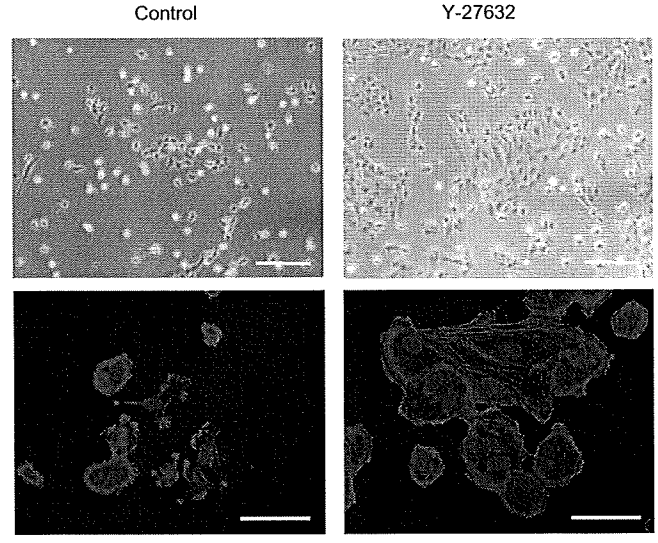

FIGURE 4. The morphologic change of passaged MCECs induced by Y-27632. *Top*: phase-contrast images of cells 24 hours after passage. *Bottom*: Immunostaining of actin in the same cells. Actin (*red*) and DAPI (*blue*). Scale bar: (**A**) 250 μm; (**B**) 50 μm.

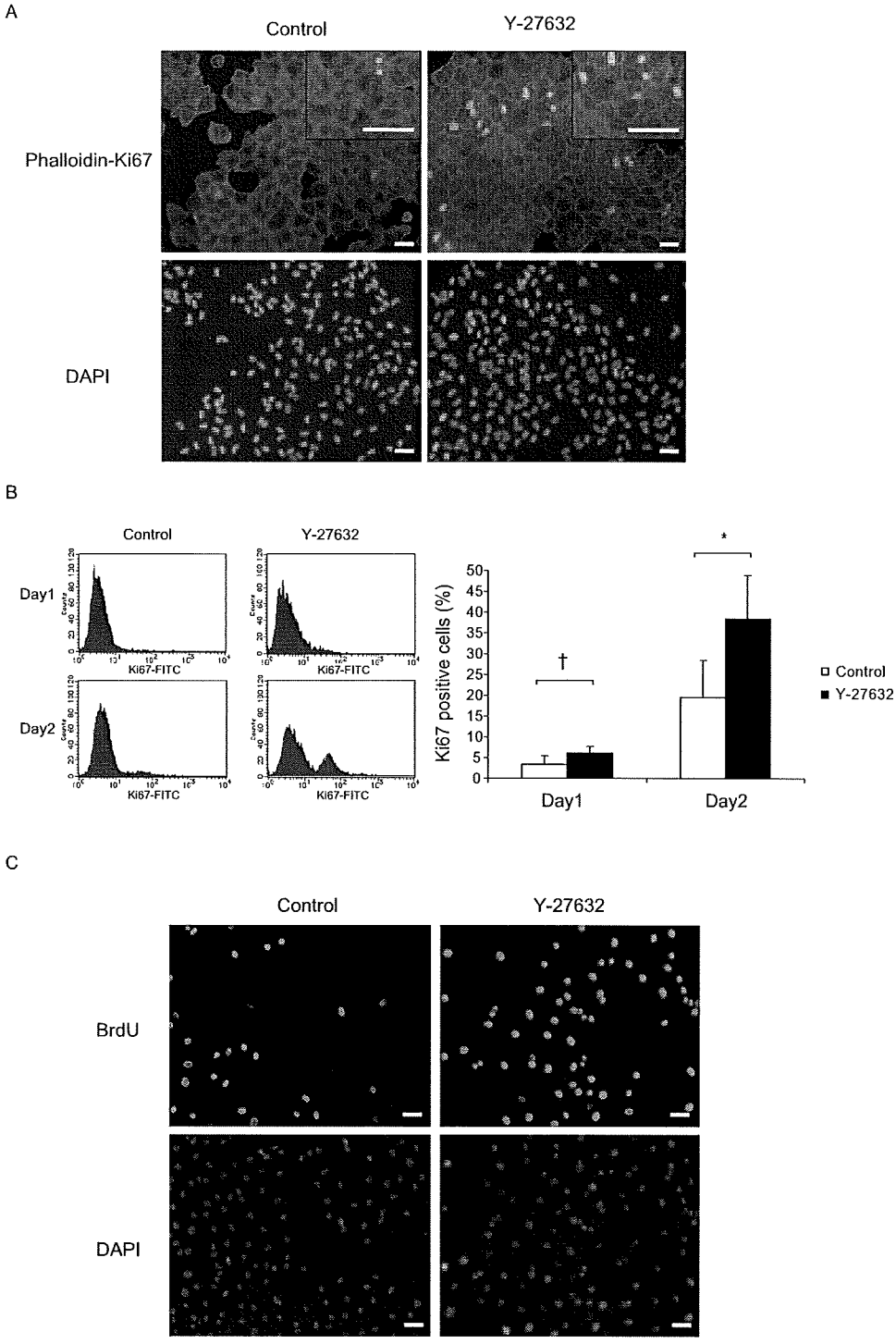

FIGURE 5. Increased frequency of proliferating MCECs by Y-27632. (**A**) Double immunostaining of Ki67 and actin fibers; the passaged MCECs were cultured for 48 hours and stained successively with Ki67 and phalloidin. Ki67 (*green*), actin (*red*), and DAPI (*blue*). *Inset*: higher magnification. (**B**) Ki67-positive cells were analyzed by flow cytometry. MCECs were subcultured for 1 or 2 days and stained successively with Ki67. The number of Ki67-positive cells was significantly elevated in the presence of Y-27632 on days 1 and 2 ($\dagger P < 0.05$, $^*P < 0.01$). Data are expressed as the mean ± SE ($n = 6$). (**C**) Y-27632 increased the frequency of BrdU-labeled MCECs. The MCECs were subcultured for 24 hours and incubated further for 24 hours with a 5-BrdU-labeling reagent, then stained with mouse anti-BrdU antibody. DAPI (*blue*). Scale bar: (**A**) 250 μm; (**C**) 100 μm.

confluence. All cells were then dissociated to single cells by trypsin digestion and recovered, including floating cells, 1 day after subculture in the presence of 10% FBS. The flow cytometry patterns of the annexin V assay revealed that Y-27632 treatment significantly decreased apoptosis ($P < 0.01$; Fig. 6A). The inhibition of apoptosis during culture without any stress load was lowered from 12.4% ± 4.6% in the control group to 2.0% ± 1.6% in the subculture group containing Y-27632, thus implicating the contribution of the apoptosis-reducing activity of Y-27632 to the efficient subculture of MCECs (Fig. 6B).

DISCUSSION

Inhibition of Rho/ROCK signaling by Y-27632 clearly promoted MCEC adhesion and inhibited apoptosis during culture. It also increased the proliferating cell population. These findings were confirmed with cynomolgus monkey-derived MCECs, which have poor proliferation potential, as do HCECs. MCECs are considered to be the preferable experimental tool for investigating nonproliferative HCECs, compared with rodent CECs or those derived from a rabbit

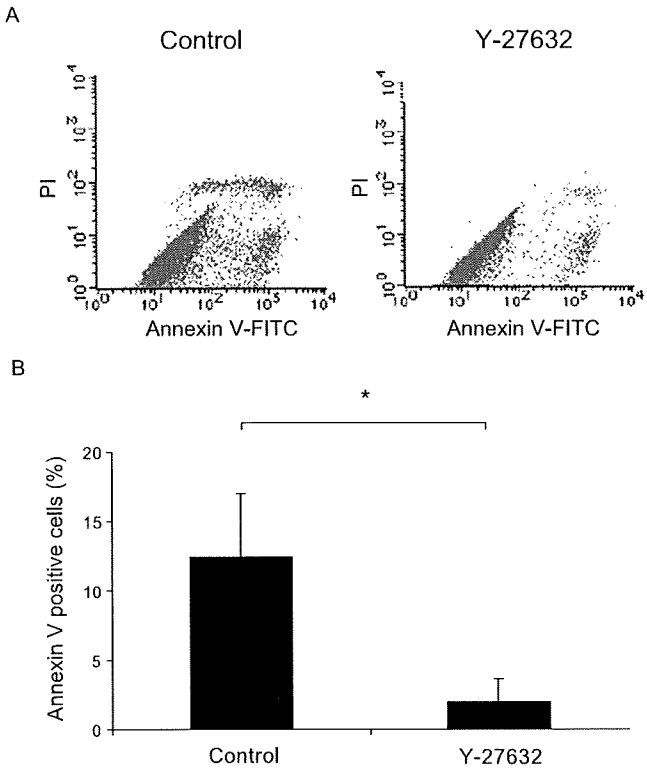

FIGURE 6. (A) Subcultured MCECs were dissociated to single cells by trypsin 24 hours after the subculture and subjected to annexin V assay. (B) The inhibition of apoptosis was lowered significantly from 12.4% ± 4.6% (control) to 2.0% ± 1.6% in the presence of Y-27632 (*$P < 0.01$). Data are expressed as the mean ± SE ($n = 4$).

in which the CECs retain a high proliferative ability both in vivo and in vitro.[7–9]

Although we found that MCECs tended to show a cell-senescence phenotype after only a few passages, we successfully cultivated and passaged MCECs in the presence of the ROCK inhibitor Y-27632. There have been several reports of successful CEC cultivation in which both explants[4,17] and cell suspensions[15] were used. There is almost no mitotic activity in the HCECs throughout the lifespan, and proliferation of adult HCECs cannot be achieved with standard cell-culturing techniques.[29] However, adult HCECs have been reported to proliferate when cultured with ECM derived from animals.[4,15,16] The fact that adult HCECs proliferate in the presence of ECM suggests that the interaction with the substratum is indispensable for the efficient growth and maintenance of MCECs.

In this context, it is of note that inhibition of the Rho/ROCK pathway by Y-27632 promotes cell adhesion to substrates of cultured THP-1 monocytes[19] and human Tenon fibroblast.[30] The actin cytoskeleton plays a critical role in cell adhesion,[19,30] which coincides well with our observation that the adhesion of cultured MCECs is promoted by Y-27632. We suspect that the enhanced adhesion by Y-27632 may be ascribable to the promotion of membrane protrusion by actin reconstitution[19,30] and to cell-to-cell adhesion by cadherin.[21] Further investigations on the underlying mechanism of the improved cell adhesion and the possible combined effect of Y-27632 with coated substrates such as ICAM-1, VCAM, collagen, fibronectin, and laminin[15,16,30] are likely to contribute much to further improvements in the efficacy of the culture of MCECs and HCECs.

Although the underlying mechanisms have yet to be thoroughly revealed, ROCK plays an important role in cell-cycle progression. ROCK activity is required for the formation of actin stress fibers that contribute to the sustained activation of Ras and the ERK mitogen-activated protein kinase (MAPK) after ligand stimulation.[31–33] In addition, RhoA promotes cell-cycle progression to S phase by regulating p27 degradation through its effect on cyclinE/CDK2 activity.[34] In HCECs, p27 is known to play a pivotal role in the negative regulation of cell-cycle progression.[11,12,35–37] However, and surprisingly, ROCK inhibition with Y-27632 promoted MCEC proliferation in our study (Fig. 5). Our finding that ROCK inhibition promotes the cell-cycle progression contrast with previously reported results.[25,31–33] This unexpected promotion of the cell-cycle progression of MCECs may be partially explained by the previous findings that the Rho/ROCK signaling, including cell proliferation, are cell-type-dependent.[38,39] It was illustrated that the blockade of sustained ERK/MAPK activity by inhibiting Rho and ROCK led to rapid cyclin-D1 induction through activation of Rac1 and Cdc42 in murine fibroblasts.[31,33] Although further studies are needed, cell adhesion and motility, which are enhanced by ROCK inhibition,[40] may have a positive effect on MCEC proliferation. Further investigations are necessary to determine whether the increased in cell proliferation observed in our studies can be ascribed to an effect on the molecular modules regulating cell-cycle progression.

ROCK is involved in the regulation of apoptosis.[38,41] Significant morphologic changes including contraction, membrane blebbing, and nuclear disintegration during apoptosis are driven by the ROCK-mediated actin-myosin contractile force.[42] ROCK inhibition has been reported to have an antiapoptotic effect in some models, such as a spinal cord injury model,[43] dissociated human embryonic stem cells,[44] and grafted neural precursors.[45] Recent research has highlighted the prosurvival effect of ROCK inhibitors for clinical use.[38] In this line, we confirmed the antiapoptotic effect of Y-27632 in cultivated MCECs. Reducing apoptotic cells during primary culture and passage procedures is beneficial, because a higher number of viable HCECs could be gained from a limited number of HCECs obtained from a donor in a clinical setting. However, ROCK inhibitors may induce apoptosis in specialized cell types,[46] including corneal epithelial cells.[47] Further research is needed to determine whether ROCK is a crucial target for these effects. The use of a ROCK $I^{-/-}$ and ROCK $II^{-/-}$ mouse model may clarify the contribution of kinase to apoptosis. HCECs with poor cell adhesion in the primary culture and in subcultures tend to show cell senescence with fibroblastic cell contamination.[16,18] Our preliminary observations indicate that MCECs assume the delayed cell-senescence phenotype during passage in the presence of Y-27632 (data not shown). Effective culture of HCECs from a limited number of donors is crucial for clinical use. Moreover, autologous CEC transplantation, obtained from a patient's fellow eye, will overcome allograft rejection. Our studies will be expanded to HCECs before clinical application, in combination with the previously reported CEC-sheet transplantation technique.[10] We predict that Y-27632 may be useful for the improved cultivation of HCECs. Of importance, no modification of the chromosome in Y-27632-treated cells has been reported,[44,48] and Y-27632, along with Fasudil, is already used clinically in cardiovascular therapies,[49] thus suggesting its safety in the clinical setting. Y-27632 is also reportedly effective in preventing fibroproliferation in glaucoma surgery[30] and as such may be an effective antiscarring agent after ocular surgery.

In summary, our results indicate that inhibition of Rho/ROCK signaling by the specific ROCK inhibitor Y-27632 promoted the adhesion of MCECs, inhibited apoptosis, and increased the frequency of proliferating cells. Our results with nonhuman primate CECs which have a low proliferative ability, similar to HCECs, raises the possibility that the ROCK inhibitor

may serve as a new tool in cultivating HCECs for newly emerging transplantation therapies.

Acknowledgments

The authors thank Yoshiki Sasai and Masatoshi Ohgushi for their assistance and invaluable advice about ROCK inhibitors and Hisako Hitora for technical assistance.

References

1. Melles GR, Lander F, Rietveld FJ. Transplantation of Descemet's membrane carrying viable endothelium through a small scleral incision. *Cornea.* 2002;21:415-418.
2. Terry MA, Ousley PJ. Deep lamellar endothelial keratoplasty in the first United States patients: early clinical results. *Cornea.* 2001;20: 239-243.
3. Price FW Jr, Price MO. Descemet's stripping with endothelial keratoplasty in 50 eyes: a refractive neutral corneal transplant. *J Refract Surg.* 2005;21:339-345.
4. Mimura T, Yamagami S, Yokoo S, et al. Cultured human corneal endothelial cell transplantation with a collagen sheet in a rabbit model. *Invest Ophthalmol Vis Sci.* 2004;45:2992-2997.
5. Ishino Y, Sano Y, Nakamura T, et al. Amniotic membrane as a carrier for cultivated human corneal endothelial cell transplantation. *Invest Ophthalmol Vis Sci.* 2004;45:800-806.
6. Sumide T, Nishida K, Yamato M, et al. Functional human corneal endothelial cell sheets harvested from temperature-responsive culture surfaces. *FASEB J.* 2006;20:392-394.
7. Mimura T, Yamagami S, Yokoo S, et al. Sphere therapy for corneal endothelium deficiency in a rabbit model. *Invest Ophthalmol Vis Sci.* 2005;46:3128-3135.
8. Mimura T, Yokoo S, Araie M, Amano S, Yamagami S. Treatment of rabbit bullous keratopathy with precursors derived from cultured human corneal endothelium. *Invest Ophthalmol Vis Sci.* 2005;46: 3637-3644.
9. Van Horn DL, Sendele DD, Seideman S, Buco PJ. Regenerative capacity of the corneal endothelium in rabbit and cat. *Invest Ophthalmol Vis Sci.* 1977;16:597-613.
10. Koizumi N, Sakamoto Y, Okumura N, et al. Cultivated corneal endothelial cell sheet transplantation in a primate model. *Invest Ophthalmol Vis Sci.* 2007;48:4519-4526.
11. Joyce NC, Harris DL, Mello DM. Mechanisms of mitotic inhibition in corneal endothelium: contact inhibition and TGF-beta2. *Invest Ophthalmol Vis Sci.* 2002;43:2152-2159.
12. Yoshida K, Kase S, Nakayama K, et al. Involvement of p27KIP1 in the proliferation of the developing corneal endothelium. *Invest Ophthalmol Vis Sci.* 2004;45:2163-2167.
13. Enomoto K, Mimura T, Harris DL, Joyce NC. Age differences in cyclin-dependent kinase inhibitor expression and rb hyperphosphorylation in human corneal endothelial cells. *Invest Ophthalmol Vis Sci.* 2006;47:4330-4340.
14. Mimura T, Joyce NC. Replication competence and senescence in central and peripheral human corneal endothelium. *Invest Ophthalmol Vis Sci.* 2006;47:1387-1396.
15. Zhu C, Joyce NC. Proliferative response of corneal endothelial cells from young and older donors. *Invest Ophthalmol Vis Sci.* 2004;45:1743-1751.
16. Engelmann K, Bohnke M, Friedl P. Isolation and long-term cultivation of human corneal endothelial cells. *Invest Ophthalmol Vis Sci.* 1988;29:1656-1662.
17. Miyata K, Drake J, Osakabe Y, et al. Effect of donor age on morphologic variation of cultured human corneal endothelial cells. *Cornea.* 2001;20:59-63.
18. Blake DA, Yu H, Young DL, Caldwell DR. Matrix stimulates the proliferation of human corneal endothelial cells in culture. *Invest Ophthalmol Vis Sci.* 1997;38:1119-1129.
19. Worthylake RA, Burridge K. RhoA and ROCK promote migration by limiting membrane protrusions. *J Biol Chem.* 2003;278:13578-13584.
20. Hall A. Rho GTPases and the actin cytoskeleton. *Science.* 1998; 279:509-514.
21. Braga VM, Del Maschio A, Machesky L, Dejana E. Regulation of cadherin function by Rho and Rac: modulation by junction maturation and cellular context. *Mol Biol Cell.* 1999;10:9-22.
22. Kaibuchi K, Kuroda S, Amano M. Regulation of the cytoskeleton and cell adhesion by the Rho family GTPases in mammalian cells. *Annu Rev Biochem.* 1999;68:459-486.
23. Somlyo AP, Somlyo AV. Signal transduction by G-proteins, rho-kinase and protein phosphatase to smooth muscle and non-muscle myosin II. *J Physiol.* 2000;522;2:177-185.
24. Nakagawa O, Fujisawa K, Ishizaki T, Saito Y, Nakao K, Narumiya S. ROCK-I and ROCK-II, two isoforms of Rho-associated coiled-coil forming protein serine/threonine kinase in mice. *FEBS Lett.* 1996; 392:189-193.
25. Olson MF, Ashworth A, Hall A. An essential role for Rho, Rac, and Cdc42 GTPases in cell cycle progression through G1. *Science.* 1995;269:1270-1272.
26. Croft DR, Olson MF. The Rho GTPase effector ROCK regulates cyclin A, cyclin D1, and p27Kip1 levels by distinct mechanisms. *Mol Cell Biol.* 2006;26:4612-4627.
27. Chen J, Guerriero E, Lathrop K, SundarRaj N. Rho/ROCK signaling in regulation of corneal epithelial cell cycle progression. *Invest Ophthalmol Vis Sci.* 2008;49:175-183.
28. Narumiya S, Ishizaki T, Uehata M. Use and properties of ROCK-specific inhibitor Y-27632. *Methods Enzymol.* 2000;325:273-284.
29. Insler MS, Lopez JG. Transplantation of cultured human neonatal corneal endothelium. *Curr Eye Res.* 1986;5:967-972.
30. Honjo M, Tanihara H, Kameda T, Kawaji T, Yoshimura N, Araie M. Potential role of Rho-associated protein kinase inhibitor Y-27632 in glaucoma filtration surgery. *Invest Ophthalmol Vis Sci.* 2007;48: 5549-5557.
31. Roovers K, Assoian RK. Effects of rho kinase and actin stress fibers on sustained extracellular signal-regulated kinase activity and activation of G(1) phase cyclin-dependent kinases. *Mol Cell Biol.* 2003;23:4283-4294.
32. Swant JD, Rendon BE, Symons M, Mitchell RA. Rho GTPase-dependent signaling is required for macrophage migration inhibitory factor-mediated expression of cyclin D1. *J Biol Chem.* 2005;280: 23066-23072.
33. Welsh CF, Roovers K, Villanueva J, Liu Y, Schwartz MA, Assoian RK. Timing of cyclin D1 expression within G1 phase is controlled by Rho. *Nat Cell Biol.* 2001;3:950-957.
34. Hu W, Bellone CJ, Baldassare JJ. RhoA stimulates p27(Kip) degradation through its regulation of cyclin E/CDK2 activity. *J Biol Chem.* 1999;274:3396-3401.
35. Kikuchi M, Zhu C, Senoo T, Obara Y, Joyce NC. p27kip1 siRNA induces proliferation in corneal endothelial cells from young but not older donors. *Invest Ophthalmol Vis Sci.* 2006;47:4803-4809.
36. Lee HT, Kay EP. Regulatory role of PI 3-kinase on expression of Cdk4 and p27, nuclear localization of Cdk4, and phosphorylation of p27 in corneal endothelial cells. *Invest Ophthalmol Vis Sci.* 2003;44:1521-1528.
37. Lee JG, Kay EP. Two populations of p27 use differential kinetics to phosphorylate Ser-10 and Thr-187 via phosphatidylinositol 3-kinase in response to fibroblast growth factor-2 stimulation. *J Biol Chem.* 2007;282:6444-6454.
38. Olson MF. Applications for ROCK kinase inhibition. *Curr Opin Cell Biol.* 2008;20:242-248.
39. Coleman ML, Marshall CJ, Olson MF. RAS and RHO GTPases in G1-phase cell-cycle regulation. *Nat Rev Mol Cell Biol.* 2004;5:355-366.
40. Croft DR, Sahai E, Mavria G, et al. Conditional ROCK activation in vivo induces tumor cell dissemination and angiogenesis. *Cancer Res.* 2004;64:8994-9001.
41. Shi J, Wei L. Rho kinase in the regulation of cell death and survival. *Arch Immunol Ther Exp (Warsz).* 2007;55:61-75.
42. Coleman ML, Olson MF. Rho GTPase signalling pathways in the morphological changes associated with apoptosis. *Cell Death Differ.* 2002;9:493-504.
43. Dubreuil CI, Winton MJ, McKerracher L. Rho activation patterns after spinal cord injury and the role of activated Rho in apoptosis in the central nervous system. *J Cell Biol.* 2003;162:233-243.

44. Watanabe K, Ueno M, Kamiya D, et al. A ROCK inhibitor permits survival of dissociated human embryonic stem cells. *Nat Biotechnol.* 2007;25:681–686.
45. Koyanagi M, Takahashi J, Arakawa Y, et al. Inhibition of the Rho/ROCK pathway reduces apoptosis during transplantation of embryonic stem cell-derived neural precursors. *J Neurosci Res.* 2008;86:270–280.
46. Moore M, Marroquin BA, Gugliotta W, Tse R, White SR. Rho kinase inhibition initiates apoptosis in human airway epithelial cells. *Am J Respir Cell Mol Biol.* 2004;30:379–387.
47. Svoboda KK, Moessner P, Field T, Acevedo J. ROCK inhibitor (Y27632) increases apoptosis and disrupts the actin cortical mat in embryonic avian corneal epithelium. *Dev Dyn.* 2004;229:579–590.
48. Kobayashi K, Takahashi M, Matsushita N, et al. Survival of developing motor neurons mediated by Rho GTPase signaling pathway through Rho-kinase. *J Neurosci.* 2004;24:3480–3488.
49. Hu E, Lee D. Rho kinase as potential therapeutic target for cardiovascular diseases: opportunities and challenges. *Expert Opin Ther Targets.* 2005;9:715–736.